# [$\bar{\text{P}}$ANDA internal note]: Fast simulation studies $p\bar{p} \rightarrow h_c \rightarrow 5\pi$

*Anastasia Karavdina, May 2014*

## 1 Current knowledge

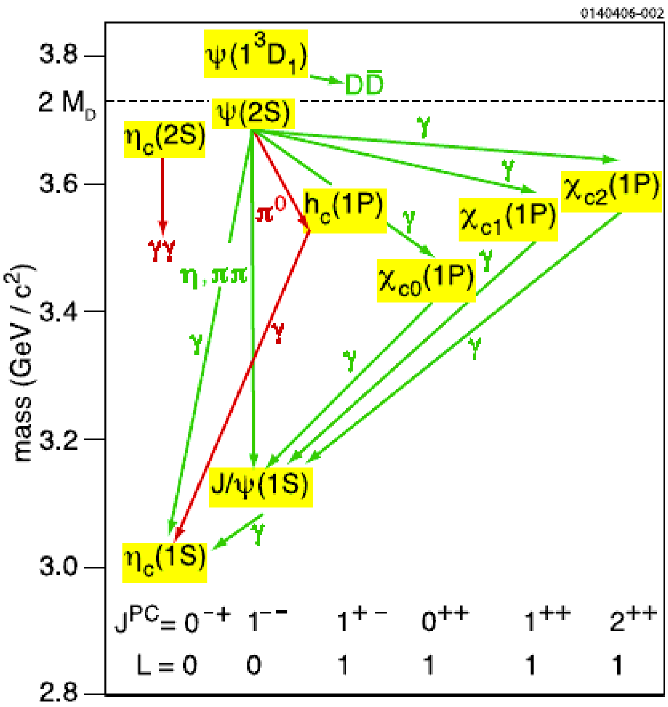


Fig. 1: Low-laying charmonium states with observed transition among them [2]

QCD-motivated potential models successfully described the $J/\psi$ and $\psi'$ as $\bar{c}c$ states soon after they were discovered. These models have stood up quite well over the ensuing years, during which time other low-lying $\bar{c}c$ states were discovered and found to have properties that agree reasonably well with the models' predictions. The levels are labeled by S, P , D, corresponding to relative orbital angular momentum $L$ = 0, 1, 2 between quark and antiquark. The spin of the quark and antiquark can couple to either $S$ = 0 (spin-singlet) or $S$ = 1 (spin-triplet) states. The parity of a quark-antiquark state with orbital angular $L$ is $P = (-1)^{L+1}$; the charge-conjugation eigenvalue is $C = (-1)^{L+S}$. Values of $J^{PC}$ are shown at the bottom if Fig. 1.

Among all so-called conventional charmonium states there are two not well established: $h_c(1P)$ and $\eta_c(2S)$).

The $h_c$ is the $^1P_1$ state of charmonium, singlet partner of the long-known $\chi_{cJ}$ triplet $^3P_J$. The spin-averaged centroid of the triplet states:

$$< m(1^3P_J) >= [m(\chi_{c0}) + 3m(\chi_{c1}) + 5m(\chi_{c2})]/9 \quad (1)$$

is expected to be near $h_c(1P)$ mass, making the hyperfine mass splitting:

$$\Delta m_{hf}[h_c(1P)] =< m(1^3P_J) > -m[h_c(1P)] \quad (2)$$

$h_c(1P)$ I^G (J^{PC}) = ?^{?} (1^{+-}) INSPIRE search

Quantum numbers are quark model prediction, $^C$ = established by $\eta_c\gamma$ decay.

| | |
|---|---|
| $h_c(1P)$ MASS | 3525.38 ±0.11 MeV (S = 1.0) |
| $h_c(1P)$ WIDTH | 0.7 ±0.4 MeV |

$h_c(1P)$ $\Gamma(\mathrm{i})\Gamma(\overline{p}p)/\Gamma(\mathrm{total})$

**Decay Modes**

| $\Gamma_i$ | Mode | Fraction ($\Gamma_i$ / $\Gamma$) | Scale Factor/ Confidence Level | P (MeV/c) |
|---|---|---|---|---|
| $\Gamma_1$ | $h_c(1P) \to J/\psi(1S)\pi^0$ | | | 382 |
| $\Gamma_2$ | $h_c(1P) \to J/\psi(1S)\pi\pi$ | not seen | | 312 |
| $\Gamma_3$ | $h_c(1P) \to p\overline{p}$ | | | 1492 |
| $\Gamma_4$ | $h_c(1P) \to \eta_c(1S)\gamma$ | $(.051 \pm .006) \times 10^1$ | | 500 |
| $\Gamma_5$ | $h_c(1P) \to \pi^+\pi^-\pi^0$ | $<2.2 \times 10^{-3}$ | | 1749 |
| $\Gamma_6$ | $h_c(1P) \to 2\pi^+ 2\pi^- \pi^0$ | $2.2^{+0.8}_{-0.7}$ % | | 1716 |
| $\Gamma_7$ | $h_c(1P) \to 3\pi^+ 3\pi^- \pi^0$ | <2.9 % | | 1661 |

Fig. 2: Current knowledge about $h_c(1P)$ (status of 2013 [1])

The hyperfine mass an important measure of the spin−spin interaction.

Data on the $c\bar{c}$ singlet state $h_c(1P)$ remains sparse and summarized on Fig. 2. More complete expectation for quantum numbers is given in [3]: $I^G(J^{PC}){=}0^-(1^{+-})$.

Dominating decay channel for $h_c(1P)$ is $h_c(1P) \to \eta_c(1S)\gamma$. By coincidence $h_c(1P) \to$ (light hadrons) has comparable rates [5].

## 2 Choose of decay mode and construction of model for this analysis

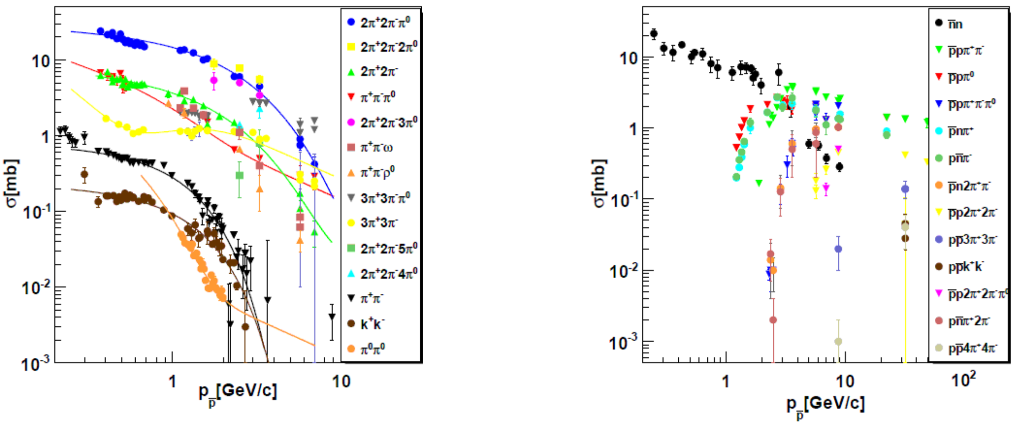


Fig. 3: Inelastic channels in $\bar{p}p$ interactions (status of 2013)

Because $h_c(1P)$ should have negative G-parity, multi-pion decay are likely to involve an odd number of pions (G is a multiplicative quantum number, so for a system of $n\pi$ G=$(-1)^n$). Interesting enough that among just 3 found mode of $h_c(1P)$ to light hadrons, only one has branching fraction measurement (and not just limit): $h_c(1P) \to 2(\pi^-\pi^+)\pi^0$. At $\bar{\text{P}}$ANDA channel $h_c(1P) \to 2(\pi^-\pi^+)\pi^0$ can be one of the most challenging, due to high cross-sections of such final states in $\bar{p}p$ interactions (Fig.3). Therefore one can expect high contamination of physical background. But also high statistic for analysis should be available during just few days of $\bar{\text{P}}$ANDA run. During time given for simulation I did not manage to reach any theory expert in the field, thus I took responsibility to construct my own naive model, which was inspired by discussions in [3] and [7].

In [3] charmonium decays via meson pair are discussed and they came to following conclusion by requiring helicities conservation (P - pseudoscalar, parity=-1; V - vector, parity=-1):

- $h_c \to$ PP (forbidden by angular momentum and parity conservation)
- $h_c \to$ PV (allowed)
- $h_c \to$ VV (forbidden to leading-twist accuracy)

One can cross-check SS, SV, SP (S - scalar, parity=+1) combinations from requirement:

$$(-1)^{J_c} P_c = (-1)^{J_1+J_2} P_1 P_2 \tag{3}$$

where $J_i$ and $P_i$ are spin and parity of the meson i.

- $h_c \to$ SS (forbidden by angular momentum and parity conservation)
- $h_c \to$ SV (forbidden by angular momentum and parity conservation)
- $h_c \to$ SP (allowed by angular momentum and parity conservation)

And for $V_p$ (pseudovector, parity +1):

- $h_c \to V_p$S (allowed by angular momentum and parity conservation)
- $h_c \to V_p$V (allowed by angular momentum and parity conservation)
- $h_c \to V_p$P (forbidden by angular momentum and parity conservation)
- $h_c \to V_pV_p$ (forbidden by angular momentum and parity conservation)

Also they note that G-parity or isospin-violating decays are not strictly forbidden since they can proceed through electromagnetic $c\bar{c}$ annihilation and may receive contributions from the isospin-violating part of QCD. The latter contributions, being related to the u-d quark mass difference, seem to be small.

Tab. 1: Allowed and forbidden modes for $h_c \to 1{+}2$

| PP | PV | VV | PS | SS | SV | $V_pS$ | $V_pV$ | $V_pP$ | $V_pV_p$ |
|---|---|---|---|---|---|---|---|---|---|
| − | + | $\epsilon$ | + | − | − | + | + | − | − |

## 2.1 $h_c \to 5\pi$

Let's try to construct the final state assuming $h_c \to$ PV or PS model ($V_p$ usually have quite complicated nature (and decay modes), therefore $h_c \to V_pV$ or $V_pS$ are skipped in this preliminary study). First of all we need decay modes of P, V and S to pions.

**Pseudoscalar**: $\eta$, $\eta^{'}$, $\eta_c(1S)$,
$\pi$(isospin=1), $K^{\pm}$(isospin=1/2), $K^0_S$(isospin=1/2), $K^0_L$(isospin=1/2), $D^{\pm}$(isospin=1/2)

- $\eta[0^+(0^{-+})] \to$

  $3\pi^0$ (32.57±0.23) %
  $\pi^+\pi^-\pi^0$ (28.1±0.34) %

- $\eta^{'}[0^+(0^{-+})] \to$

  $\pi^+\pi^-\pi^0$ $(3.6^{+1.1}_{-0.9}) \times 10^{-3}$
  $3\pi^0$ $(1.68\pm0.22) \times 10^{-3}$

- $K^{\pm}[\frac{1}{2}(0^-)] \to$

  $\pi^+\pi^0$ (20.66±0.08) %
  $2\pi^+\pi^-$ (5.59±0.04) %
  $\pi^+2\pi^0$ (1.761±0.022) %

- $K^0_S[\frac{1}{2}(0^-)] \to$

  $\pi^+\pi^-$ (69.20±0.05) %
  $\pi^0\pi^0$ (30.69±0.05) %
  $\pi^+\pi^-\pi^0$ $(3.5^{+1.1}_{-0.9}) \times 10^{-7}$

- $K^0_L[\frac{1}{2}(0^-)] \to$

  $3\pi^0$ (19.52±0.12) %
  $\pi^+\pi^-\pi^0$ (12.54±0.05) %

- $D^{\pm}[\frac{1}{2}(0^-)] \to$

  $\pi^+\pi^-$ $(1.26\pm0.09) \times 10^{-3}$

$\eta_c(1S)$ has $2(\pi^+\pi^-)$ and $3(\pi^+\pi^-)$ decay modes, therefore could be responsible for more multi-pion decay.

**Scalar**: $f_0$, $\chi_{c0}(1P)$
$a_0$ (isospin=1)

- $f_0(600, 980)[0^+(0^{++})] \rightarrow$

  $\pi\pi$ (dominant)

- $f_0(1500)[0^+(0^{++})] \rightarrow$

  $\pi\pi$ (34.9±2.3) %

- $\chi_{c0}(1P)[0^+(0^{++})] \rightarrow$

  $\pi\pi$ (8.4±0.4) $\times$ $10^{-3}$

$a_0$ has dominant mode $\eta\pi$ therefore could be responsible for more multi-pion decay.
$\chi_{c0}(1P)$ has 2($\pi^+\pi^-$) and 3($\pi^+\pi^-$) decay modes, therefore could be responsible for more multi-pion decay too.

**Vector**: $\omega$, $\phi$, J/$\psi$(1S)
$\rho$(isospin=1), K*(isospin=1/2), D*(isospin=1/2)

- $\omega[0^-(1^{--})] \rightarrow$

  $\pi^+\pi^-\pi^0$ (89.2±0.7) %
  $\pi^+\pi^-$ ($1.53^{+0.11}_{-0.13}$) %

- $\phi[0^-(1^{--})] \rightarrow$
  has dominate mode to $K^+K^-$

  $\pi^+\pi^-$ (7.4±1.3) $\times$ $10^{-5}$

- $\rho[1^+(1^{--})] \rightarrow$

  $\pi^+\pi^-$ (~100) %

- $K^*[\frac{1}{2}(1^-)] \rightarrow$
  $K^*$ has $K\pi$ dominate mode therefore could be responsible for more multi-pion decay.

- $D^*[\frac{1}{2}(1^-)] \rightarrow$
  $D^*$ has dominate decay modes $D\pi$ therefore could be responsible for more multi-pion decay.

Possible combinations for $h_c \rightarrow 2(\pi^+\pi^-)\pi^0$ or $h_c \rightarrow \pi^+\pi^-3\pi^0$:

- $h_c \rightarrow \eta\omega(OK), \eta\rho(violate\ isospin)$ (PV)
- $h_c \rightarrow \eta f_0(violate\ G-parity)$ (PS)

There difference between these 2 final state would be in decay mode of $\eta$. Also one should note that only $h_c \rightarrow \eta\omega$ is fully allowed.

## 2.2 Branching ratios calculation

### 2.2.1 $\mathbf{h}_c \to 2(\pi^+\pi^-)\pi^0$

PHSP:

$$Br(p\bar{p} \to h_c \to 2(\pi^+\pi^-)\pi^0) = Br(h_c \to 2(\pi^+\pi^-)\pi^0) = 2\% \tag{4}$$

$\eta\omega$:

$$\begin{aligned} Br(p\bar{p} \to h_c \to \eta\omega \to 2(\pi^+\pi^-)\pi^0) = \\ &= Br(h_c \to \eta\omega) \times Br(\eta \to \pi^+\pi^-\pi^0) \times Br(\omega \to \pi^+\pi^-) \\ &= Br(h_c \to \eta\omega) \times 0.281 \times 0.0153 = Br(h_c \to \eta\omega) \times 0.0043 \end{aligned} \tag{5}$$

$\eta\rho$:

$$\begin{aligned} Br(p\bar{p} \to h_c \to \eta\rho \to 2(\pi^+\pi^-)\pi^0) = \\ &= Br(h_c \to \eta\rho) \times Br(\eta \to \pi^+\pi^-\pi^0) \times Br(\rho \to \pi^+\pi^-) \\ &= Br(h_c \to \eta\rho) \times 0.281 \times 1 = Br(h_c \to \eta\rho) \times 0.281 \end{aligned} \tag{6}$$

$\eta f_0$:

$$\begin{aligned} Br(p\bar{p} \to h_c \to \eta f_0 \to 2(\pi^+\pi^-)\pi^0) = \\ &= Br(h_c \to \eta f_0) \times Br(\eta \to \pi^+\pi^-\pi^0) \times Br(f_0 \to \pi^+\pi^-) \\ &= Br(h_c \to \eta f_0) \times 0.281 \quad (f_0(600), f_0(980)) \\ &\text{or} \\ &= Br(h_c \to \eta f_0(1500)) \times 0.098 \quad (f_0(1500)) \end{aligned} \tag{7}$$

Assuming we know $\sigma_{cs}(p\bar{p} \to h_c)$ and $Br(h_c \to \eta\omega) = 1$, $Br(h_c \to \eta\rho) = \alpha^2 = 5.3 \times 10^{-5}$, $Br(h_c \to \eta f_0) = ???$

$\eta\omega$:

$$Br(p\bar{p} \to h_c \to \eta\omega \to 2(\pi^+\pi^-)\pi^0) = 4.3 \times 10^{-3} \tag{8}$$

$\eta\rho$:

$$Br(p\bar{p} \to h_c \to \eta\rho \to 2(\pi^+\pi^-)\pi^0) = 1.5 \times 10^{-5} \tag{9}$$

$\eta f_0$:

$$\begin{aligned} Br(p\bar{p} \to h_c \to \eta f_0 \to 2(\pi^+\pi^-)\pi^0) = \\ &= 0.28 \times Br(h_c \to \eta f_0)(f_0(600), f_0(980)) \\ &\text{or} \\ &= 9.8 \cdot 10^{-2} \times Br(h_c \to \eta f_0) = (f_0(1500)) \end{aligned} \tag{10}$$

### 2.2.2 $\mathbf{h}_c \to \pi^+\pi^-3\pi^0$

$$\begin{aligned} Br(p\bar{p} \to h_c \to \eta\omega \to \pi^+\pi^-3\pi^0) = \\ &= Br(h_c \to \eta\omega) \times Br(\eta \to 3\pi^0) \times Br(\omega \to \pi^+\pi^-) \\ &= Br(h_c \to \eta\omega) \times 0.3257 \times 0.0153 = Br(h_c \to \eta\omega) \times 0.00498 \end{aligned} \tag{11}$$

### 2.2.3 Input for significance calculation

Expected cross-section 10-100 nb.

According to estimations given above, values Br($p\bar{p} \to h_c \to 2(\pi^+\pi^-)\pi^0$) = $4\times10^{-3}$ and Br($p\bar{p} \to h_c \to \pi^+\pi^-3\pi^0$) = $5\times10^{-3}$ were used for calculation of significance.

### 2.2.4 Estimation of background

In energy range close to $h_c$ mass cross-section of $p\bar{p} \to 2(\pi^+\pi^-)\pi^0 \sim 1$ mb, assuming signal cross-section 100 nb $\Rightarrow$ signal/bkg $\sim 10^{-4}$.

For simulation with DPM (inelastic mode only): Total inelastic cross-section is $\sim 50$ mb $\Rightarrow$ signal/bkg $\sim 2\cdot10^{-6}$.

$p\bar{p} \to \pi^+\pi^-3\pi^0$ is not know, but expected to be $\sim 0.1$ mb.

# 3 Simulation Models

noPhotos, standart decay and particle file in EvtGen, only width of $h_c$ set to 0.7 MeV (mass of $h_c$ is set to 3.52593 GeV by default).For more realistic $\pi^0$ simulation *MergeNeutralClusters()* was switched on.

Following models were used for angular distribution description:

- $p\bar{p} \rightarrow h_c \rightarrow 2(\pi^+\pi^-)\pi^0$ with PHSP
- $p\bar{p} \rightarrow h_c$

  $h_c \rightarrow \eta\omega$ (HELAMP)
  $\eta \rightarrow \pi^+\pi^-\pi^0$ (PTO3P)
  $\omega \rightarrow \pi^+\pi^-$ (VSS)
- $p\bar{p} \rightarrow h_c$

  $h_c \rightarrow \eta\rho$ (HELAMP)
  $\eta \rightarrow \pi^+\pi^-\pi^0$ (PTO3P)
  $\rho \rightarrow \pi^+\pi^-$ (VSS)
- $p\bar{p} \rightarrow h_c$

  $h_c \rightarrow \eta f_0$ (HELAMP)
  $\eta \rightarrow \pi^+\pi^-\pi^0$ (PTO3P)
  $f_0 \rightarrow \pi^+\pi^-$ (HELAMP)

And similar for $h_c \rightarrow \pi^+\pi^-3\pi^0$:

- $p\bar{p} \rightarrow h_c \rightarrow \pi^+\pi^-3\pi^0$ with PHSP
- $p\bar{p} \rightarrow h_c$

  $h_c \rightarrow \eta\omega$ (HELAMP)
  $\eta \rightarrow 3\pi^0$ (PTO3P)
  $\omega \rightarrow \pi^+\pi^-$ (VSS)

where HELAMP stands for helisity amplitude, VSS means vector to scalar-scalar and PTO3P is name for pseudoscalar to 3 pseudoscalar decay model in EvtGen [8]. Weights in HELAMP and PTO3P were set to 1.0.

In the analysis $\pi^0$ was reconstructed from photons as $\pi^0 \rightarrow 2\gamma$. One should note small signal reduction due to different $\pi^0$ decay mode (Fig. 4).

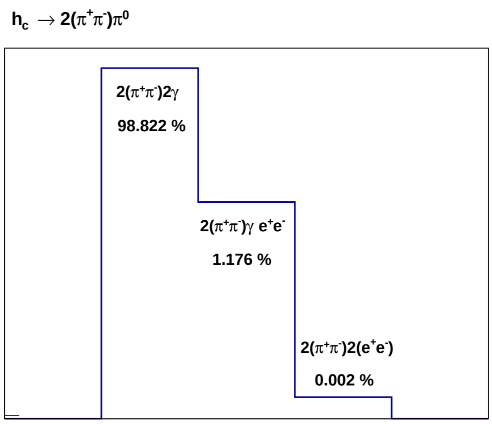


Fig. 4: Efficiency loss due to different final state (PHSP model)

Also pure PHSP model for $h_c \rightarrow \pi^+\pi^-3\pi^0$ and $h_c \rightarrow 2(\pi^+\pi^-)\pi^0$ was generated (without intermediate resonances) to compare results with particular angular model(s).

# 4 Detector model

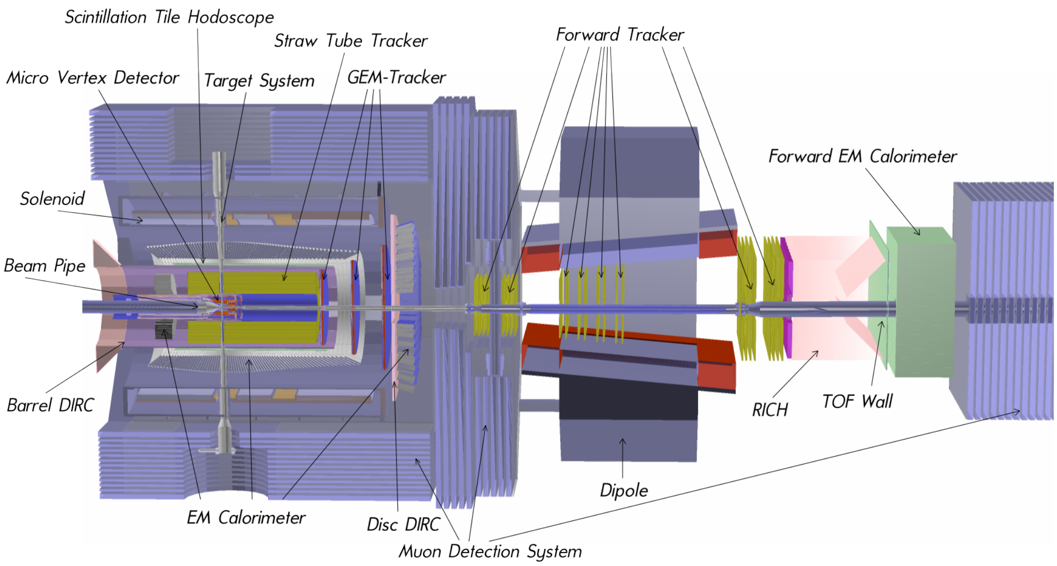


Fig. 5: Panda subsystems used in simulation with PANDAroot

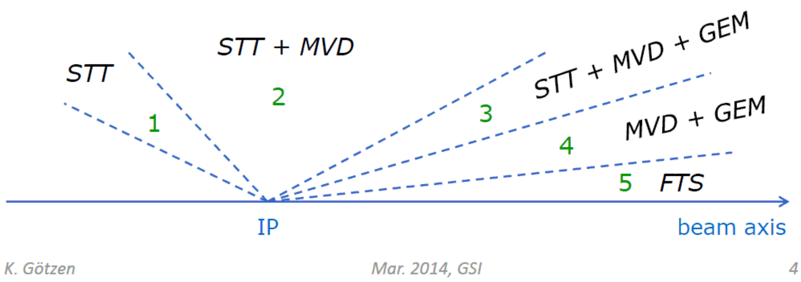


Fig. 6: Tracking systems in FastSim

Default available options:

- MvdGem (or 1) : Enable MVD and GEM for central tracking in addition to STT
- EmcBarrel (or 2) : Enable EMC barrel for calorimetry (neutral detection and PID component)
- Drc (or 3) : Enable Barrel DIRC for PID
- Dsc (or 4) : Enable Disc DIRC for PID
- FwdSpec (or 5) : Enable complete Forward Spectrometer (= Fwd Spec. EMC, Fwd Tracking, RICH, Fwd MUO)

Proposed scenarios:

I MvdGem, EmcBarrel, Drc, Dsc, FwdSpec

II MvdGem, Drc, Dsc , FwdSpec (w/o EMC)

III MvdGem, EmcBarrel, Drc, Dsc (w/o FwdSpec)

IV MvdGem, EmcBarrel, Drc, FwdSpec (w/o Disc DIRC)

V EmcBarrel, Drc, Dsc, FwdSpec (STT only)

Therefore in the main study EmcFwd, EmcBw, STT, Barrel MUO were always enabled.

# 5 Analysis

Analysis contains following steps:

- Select all charged pions (PID ALL is applied)
- Construct $\pi^0$ candidate from $2\gamma$ (and select candidate with 0.05 MeV $\pi^0$ mass window)
- Select events with required number of charged and neutral pions (e.g for $h_c \to 2(\pi^+\pi^-)\pi^0$ 2 positive, 2 negative and one neutral pions are required)
- Construct $h_c$ candidate
- Apply 4C fit
- Select event if $\chi^2$<20. In case of several candidates, pick up one with the smallest $\chi^2$

## 5.1 Model based analysis

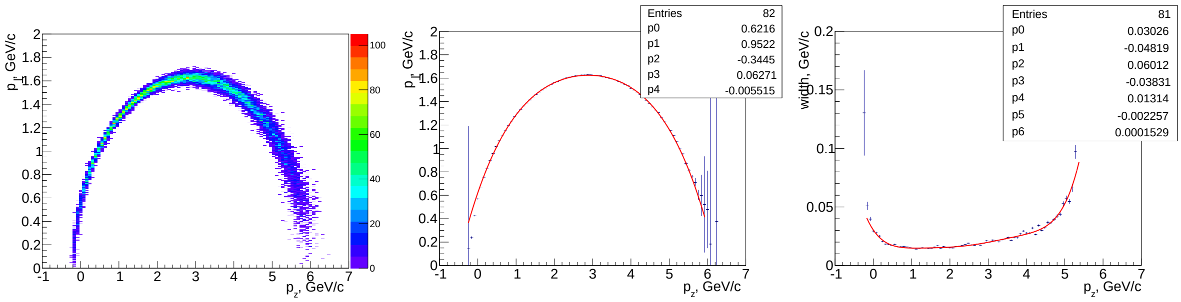


Fig. 7: Cut $p_\perp(p_z)$ for $\omega$

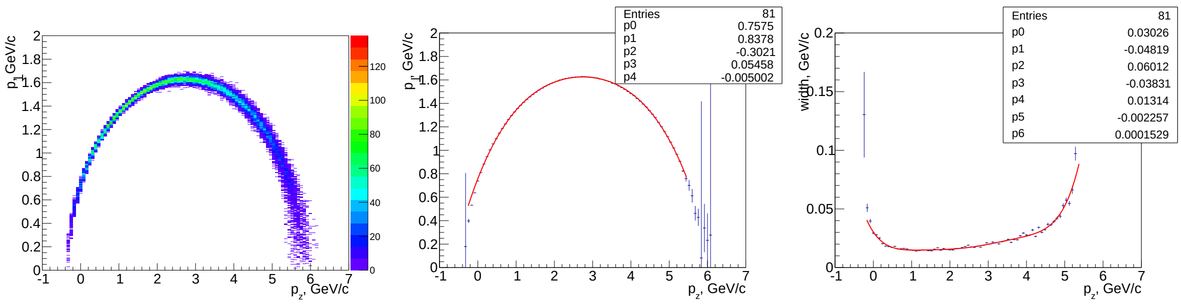


Fig. 8: Cut $p_\perp(p_z)$ for $\eta$

In the simulation we can use advantage of knowing exact model used in simulation and try to catch some signal features thanks to underlying model. For our model $h_c \to$ PV, PS one can try to reconstruct intermediate resonances ($\eta$ for P, $\omega$ or $\rho$ for V and $f_0$ for S).

We will start with $h_c \to \eta\omega$ as an example. But similar arguments are applied to any intermediate resonance combination. Both $\eta$ and $\omega$ have certain distribution in phase-space, which is visible for example on Peyrou diagram: $p_\perp(p_z)$ dependencies (Fig. 7, 8). Such kind of cut helps to get rid from combinatorical background (Fig. 9) as well as from physical background. For more stronger background suppression mass cut on intermediate states were applied. Example of mass cut is shown of Fig. 13.

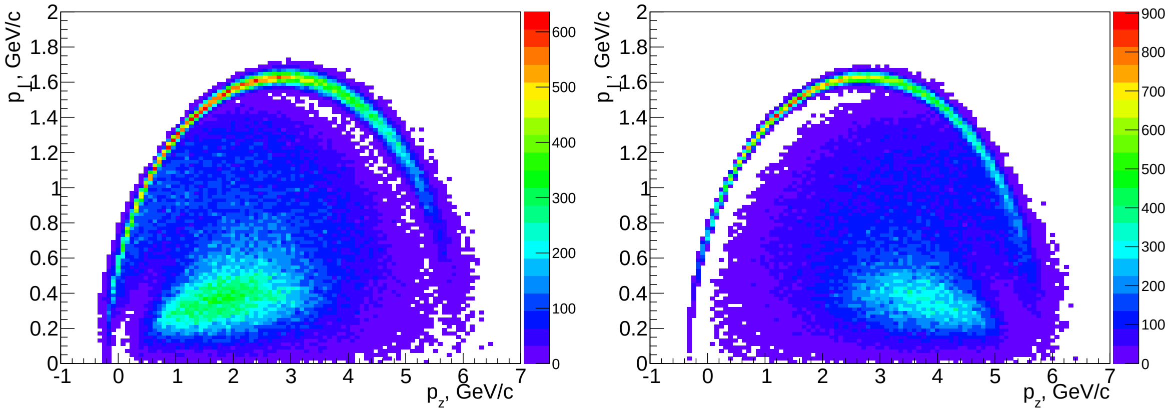


Fig. 9: Combinatorical background for $\omega$(left) and $\eta$ (right) on Peyrou diagram

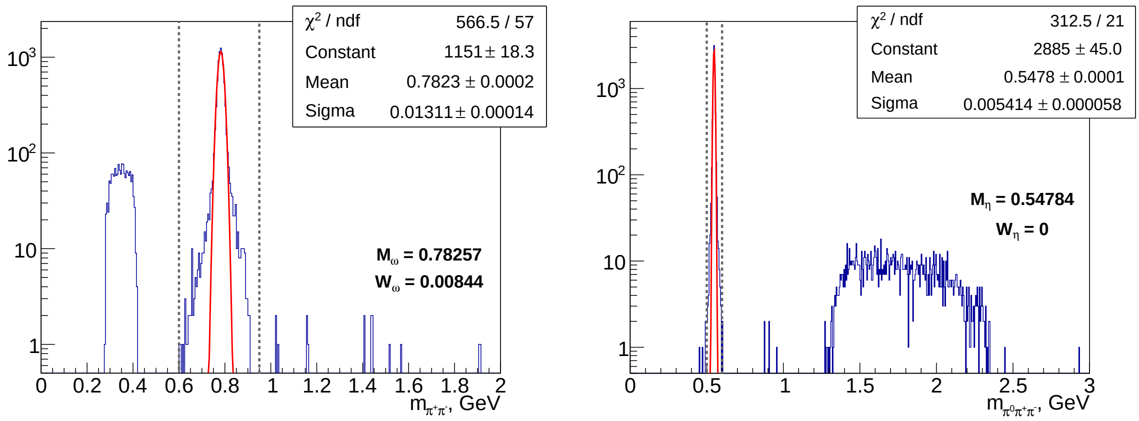


Fig. 10: Mass window cut on $\omega$ (left) and $\eta$ (right)

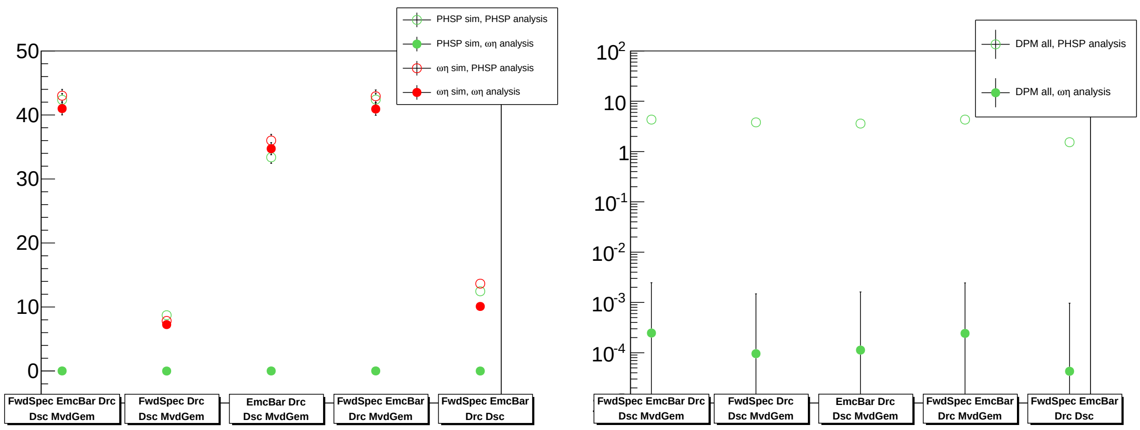


Fig. 11: Efficiency of signal (left) and background (right) reconstruction with tight cuts on $\omega\eta$

By such cut combination one can keep signal efficiency on the level of $\sim 45\%$ and reduce background to level $\sim 10^{-6}$ (Fig. 11).

Disadvantage of this method is needed extension of cuts if one would like to include more resonances. For example if not only $\eta\omega$, but also $\eta\rho$ contribution is considered. Fig. 12 illustrates difference between parameters of Peyrou diagrams for cases $\eta\omega$ and $\eta\rho$. Mass cut window also should be extended to be sure that both $\omega$ and $\rho$ are included.

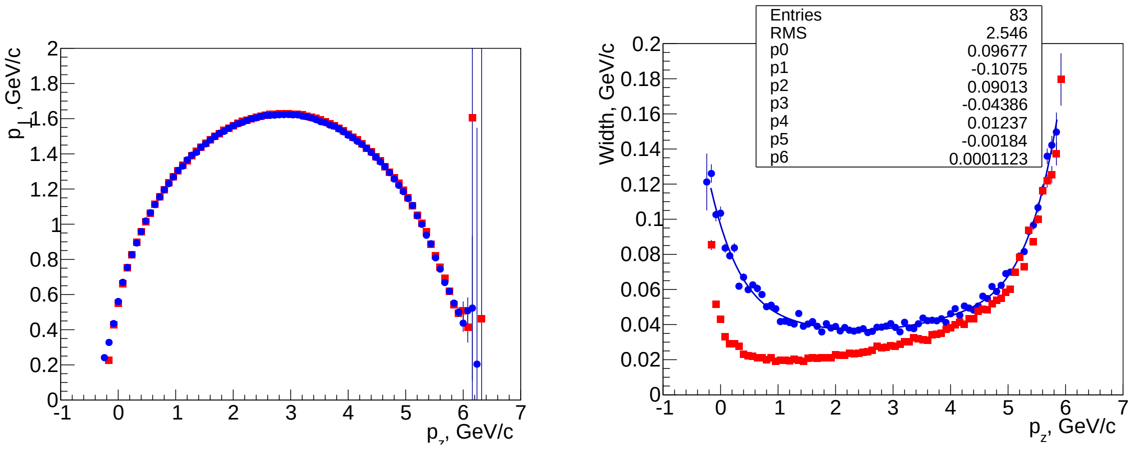


Fig. 12: Difference in cut $p_\perp(p_z)$ for $\omega$(red) and $\rho$(blue) (due to different widths?)

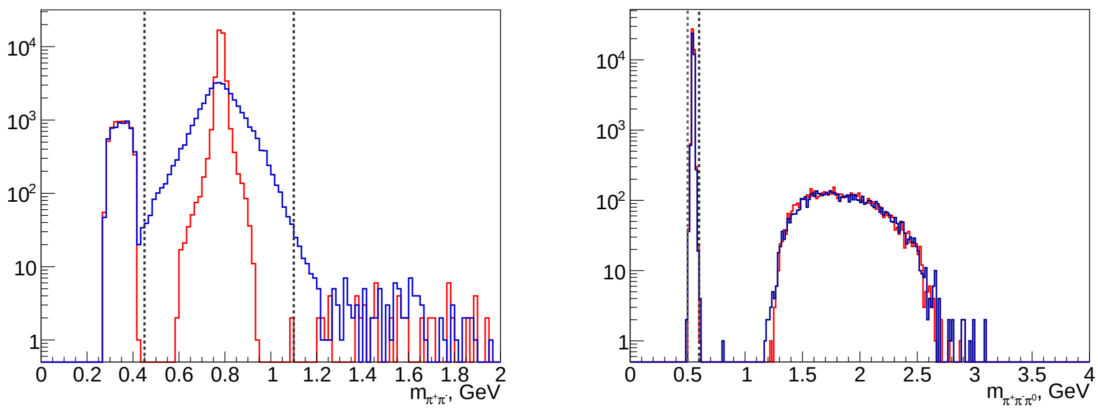


Fig. 13: Mass window cut on $\omega$&$\rho$ (left) and $\eta$ (right)

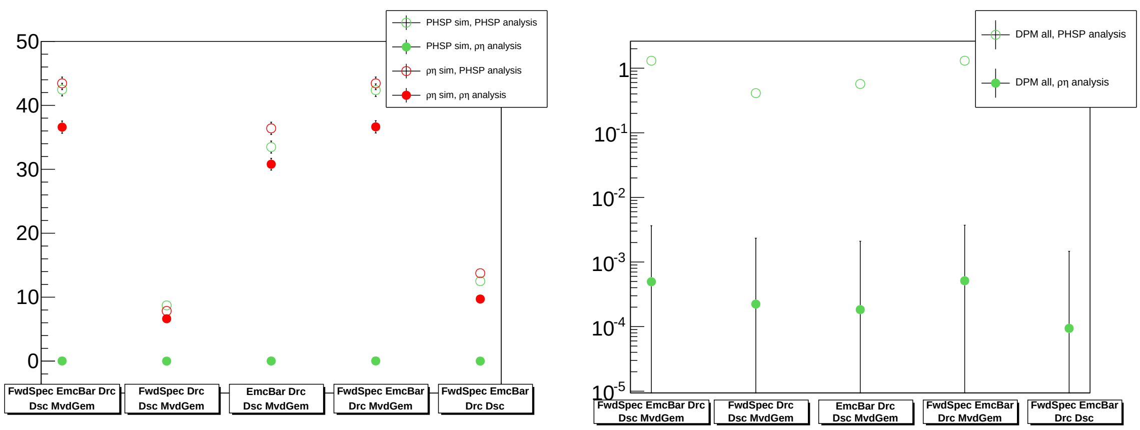


Fig. 14: Efficiency of signal (left) and background (right) reconstruction with cuts on $\rho\eta$

This extension leads to increasing background efficiency up to $\sim 10^{-5}$.

Correction of cuts become even more complicated if one would like to add $\eta f_0$ contribution (Fig. 15). And although this method seems to be very useful for physical background suppression (Fig. 16), less model dependent method becomes more preferable. According to our model $\eta$ should contribute in each case. As one can see by two tails of $p_\perp(p_z)$ on Fig. 16 (right) Peyrou distribution of $\eta$ is strongly partner dependent. Therefore only mass cut can be applied: $0.25<M^2_{3\pi}<0.35$

Applying mass cut on $2\pi$ pair doesn't make too much sense since here much more resonances can contribute (Fig. 17)

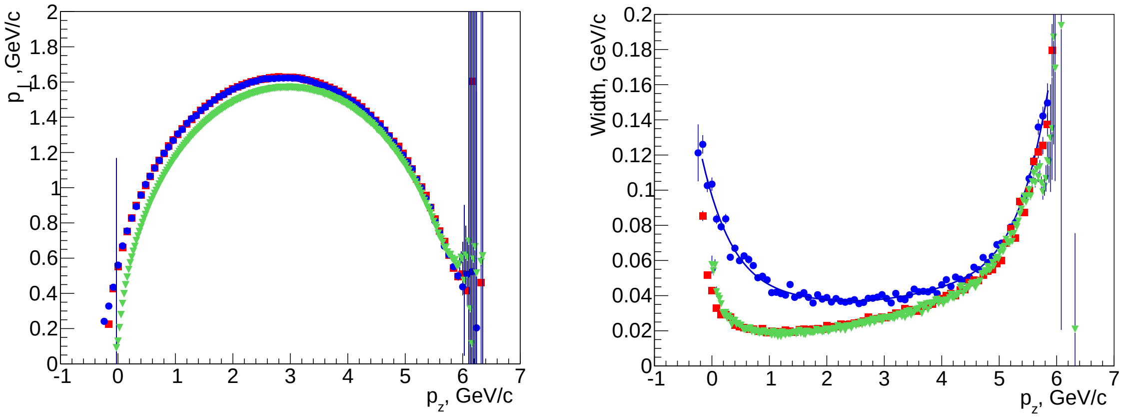


Fig. 15: Difference in cut $p_\perp(p_z)$ for $\omega$(red) and $\rho$(blue) and $f_0(980)$(green)

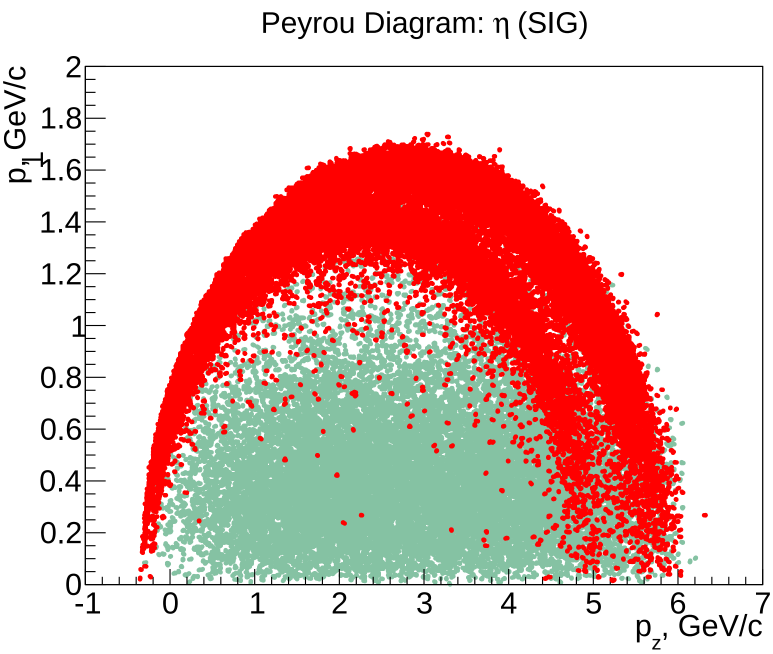


Fig. 16: DPM background (green) and signal (red) for $\eta$ on Peyrou diagram

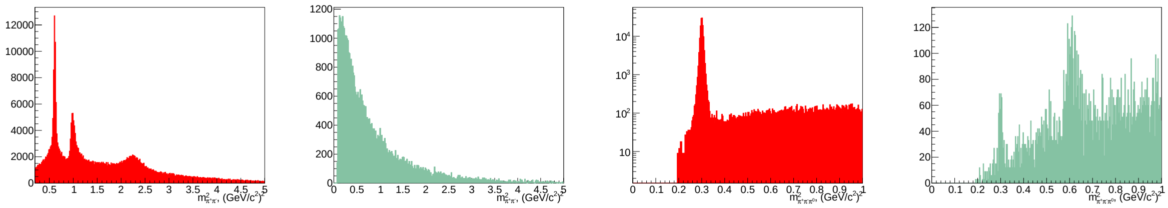

Fig. 17: From left to right: Signal(red) with $\omega$, $\rho$ and $f_0$ for $m^2$ of $\pi^+\pi^-$ combination, DPM background (green) for $m^2$ of $\pi^+\pi^-$ combination; Signal with $\eta$ contribution to $\pi^+\pi^-\pi^0$, DPM background for $m^2$ of $\pi^+\pi^-\pi^0$

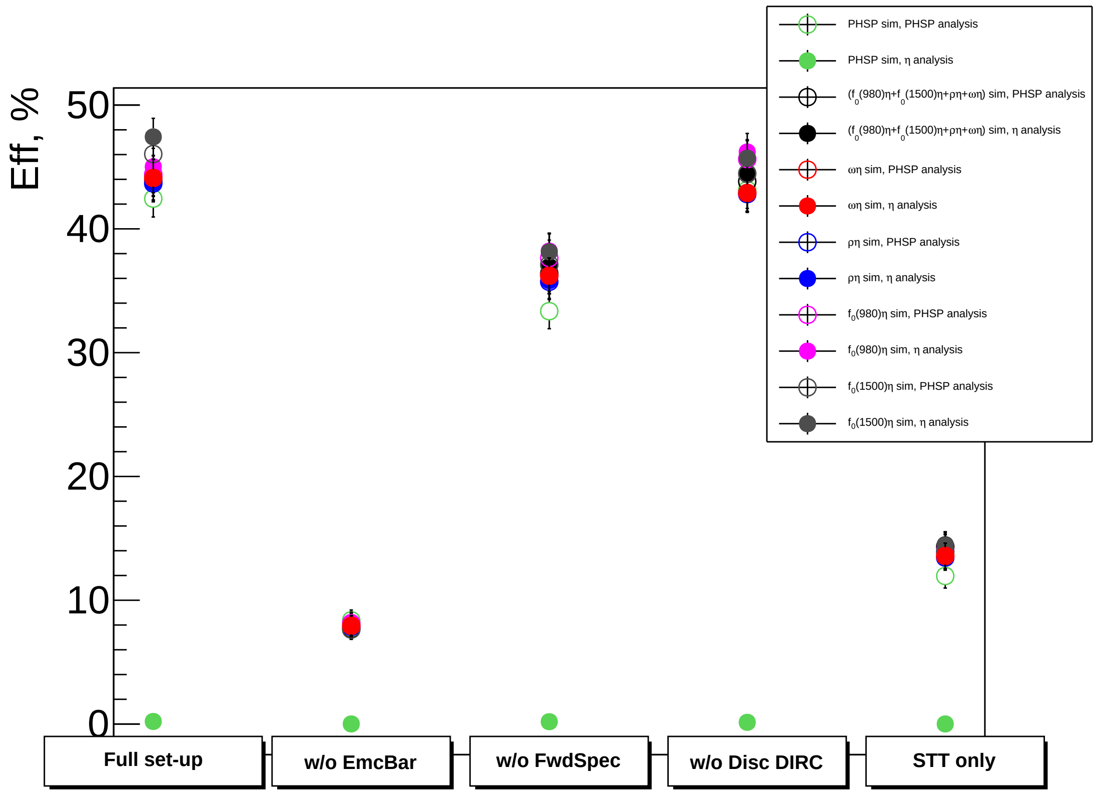


Fig. 18: Efficiency of signal reconstruction for $h_c \to 2(\pi^+\pi^-)\pi^0$ with cuts on η

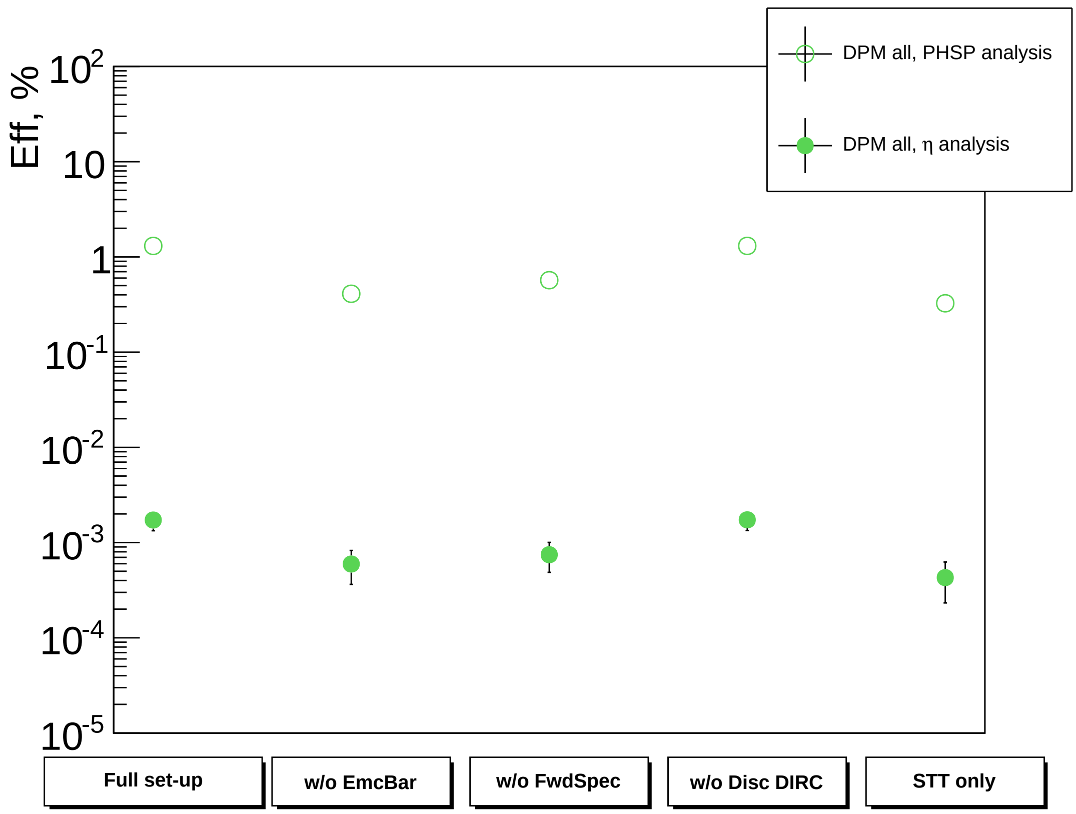


Fig. 19: Efficiency of background reconstruction for $h_c \to 2(\pi^+\pi^-)\pi^0$ with cuts on η

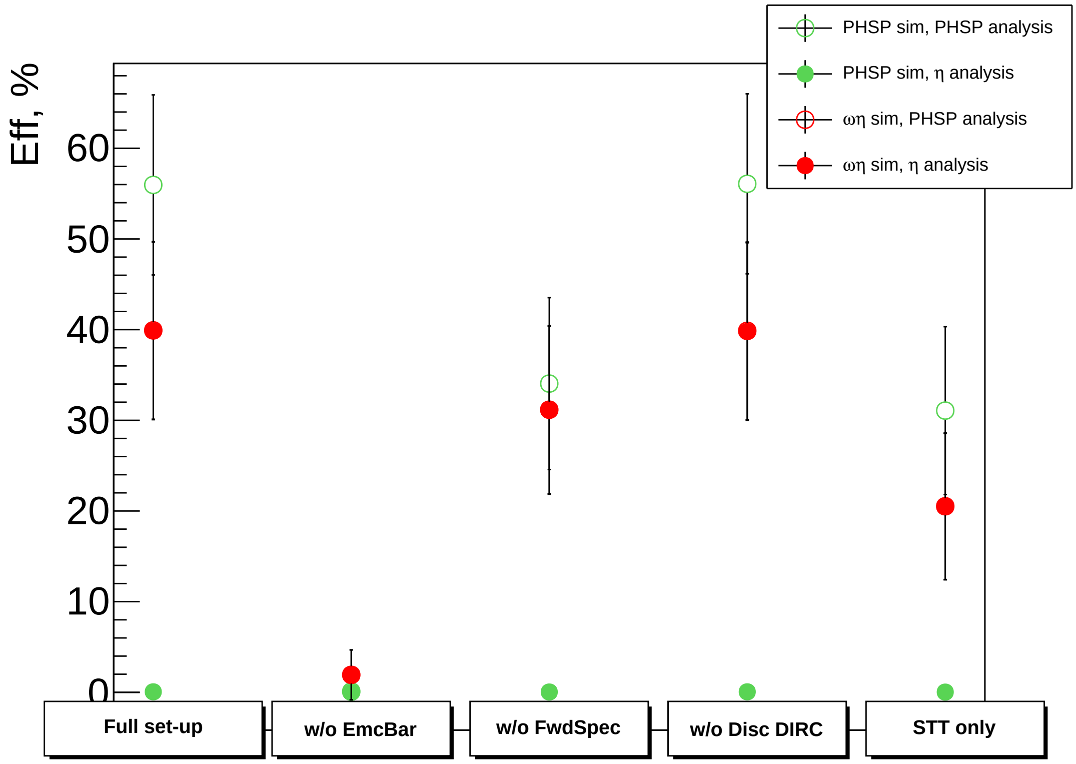


Fig. 20: Efficiency of signal reconstruction for $h_c \to \pi^+\pi^-3\pi^0$ with cuts on η

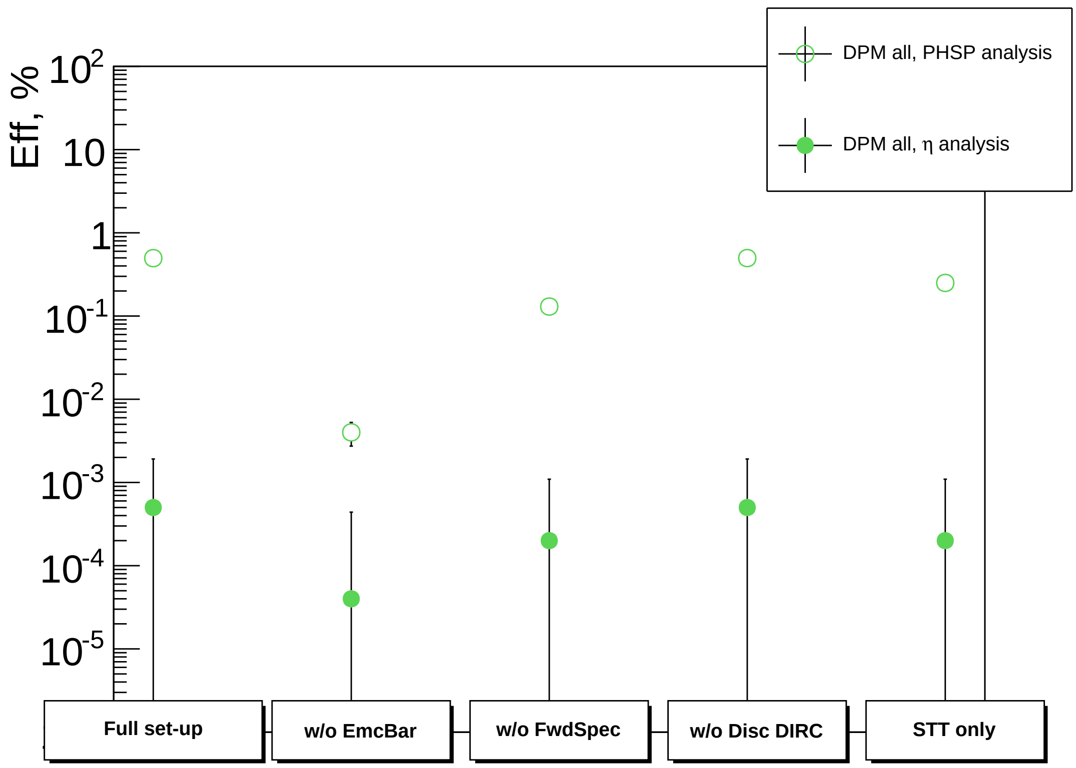


Fig. 21: Efficiency of background reconstruction for $h_c \to \pi^+\pi^-3\pi^0$ with cuts on η

Tab. 2: Efficiency (,%) for $h_c \to 2(\pi^+\pi^-)\pi^0$ signal with different (standart) detector set-ups and simulation and analysis models

| Channel Model | Analysis Model | Full | w/o EmcBar | w/o FwdSpec | w/o Disc DIRC | STT only |
|---|---|---|---|---|---|---|
| PHSP | PHSP | 42.44 | 8.38 | 33.35 | 43.14 | 11.96 |
| PHSP | $\eta$-cut | 0.21 | 0.01 | 0.19 | 0.14 | 0.01 |
| $\eta f_0(1500)$, $\eta f_0(980)$, $\eta\rho$, $\eta\omega$ | PHSP | 43.83 | 7.69 | 36.38 | 43.83 | 14.32 |
| $\eta f_0(1500)$, $\eta f_0(980)$, $\eta\rho$, $\eta\omega$ | $\eta$-cut | 44.18 | 7.79 | 36.95 | 44.39 | 14.48 |
| $\eta\omega$ | PHSP | 44.11 | 7.94 | 36.21 | 42.9 | 13.58 |
| $\eta\omega$ | $\eta$-cut | 44.11 | 7.96 | 36.2 | 42.89 | 13.59 |
| $\eta\rho$ | PHSP | 43.67 | 7.85 | 35.73 | 42.81 | 13.45 |
| $\eta\rho$ | $\eta$-cut | 43.74 | 7.86 | 35.82 | 42.91 | 13.51 |
| $\eta f_0(980)$ | PHSP | 44.4 | 8.13 | 37.64 | 45.63 | 13.97 |
| $\eta f_0(980)$ | $\eta$-cut | 45.01 | 8.21 | 38.2 | 46.21 | 14.24 |
| $\eta f_0(1500)$ | PHSP | 46.04 | 7.64 | 37.11 | 44.47 | 13.91 |
| $\eta f_0(1500)$ | $\eta$-cut | 47.43 | 7.85 | 38.14 | 45.71 | 14.45 |

Tab. 3: Efficiency (,%) for $h_c \to 2(\pi^+\pi^-)\pi^0$ background with different (standart) detector set-ups and simulation and analysis models

| Channel | Analysis Model | Full | w/o EmcBar | w/o FwdSpec | w/o Disc DIRC | STT only |
|---|---|---|---|---|---|---|
| DPM all | PHSP | 1.30 | 0.41 | 0.57 | 1.31 | 0.33 |
| DPM all | $\eta$-cut | $2\cdot10^{-3}$ | $6\cdot10^{-4}$ | $7\cdot10^{-4}$ | $2\cdot10^{-3}$ | $4\cdot10^{-4}$ |

Tab. 4: Efficiency (,%) for $h_c \to \pi^+\pi^-3\pi^0$ signal with different (standart) detector set-ups and simulation and analysis models

| Channel Model | Analysis Model | Full | w/o EmcBar | w/o FwdSpec | w/o Disc DIRC | STT only |
|---|---|---|---|---|---|---|
| PHSP | PHSP | 55.96 | 0.09 | 34.05 | 56.08 | 31.07 |
| PHSP | $\eta$-cut | 0.06 | 0.002 | 0.04 | 0.06 | 0.03 |
| $\eta\omega$ | PHSP | 39.92 | 1.93 | 31.17 | 39.87 | 20.52 |
| $\eta\omega$ | $\eta$-cut | 39.86 | 1.93 | 31.11 | 39.79 | 20.48 |

Tab. 5: Efficiency (,%) for $h_c \to \pi^+\pi^-3\pi^0$ background with different (standart) detector set-ups and simulation and analysis models

| Channel | Analysis Model | Full | w/o EmcBar | w/o FwdSpec | w/o Disc DIRC | STT only |
|---|---|---|---|---|---|---|
| DPM all | PHSP | 0.496 | 0.004 | 0.13 | 0.497 | 0.25 |
| DPM all | $\eta$-cut | $5\cdot10^{-4}$ | $4\cdot10^{-5}$ | $2\cdot10^{-4}$ | $5\cdot10^{-4}$ | $2\cdot10^{-4}$ |

# 6 Significance

Following definition of significance is used:

$$Significance(t) = \sqrt{L \cdot t} \frac{\sigma_s \cdot \epsilon_s \cdot f_{BR}}{\sqrt{\sigma_s \cdot \epsilon_s \cdot f_{BR} + \sigma_b \cdot \epsilon_b}} \tag{12}$$

where there are "known" parameters:

$\sigma_s$ – signal cross-section (10-100 nb)
$\sigma_b$ – bkg cross-section (50 mb)
$f_{BR}$ – BR factor for given decay (0.004 for $h_c \to 2(\pi^+\pi^-)\pi^0$, 0.005 for $h_c \to \pi^+\pi^-3\pi^0$)
$L$ – luminosity ($10^{32}$)

and "input" parameters:

$\epsilon_s$ – rec. efficiency for signal
$\epsilon_b$ – rec. efficiency for bkg

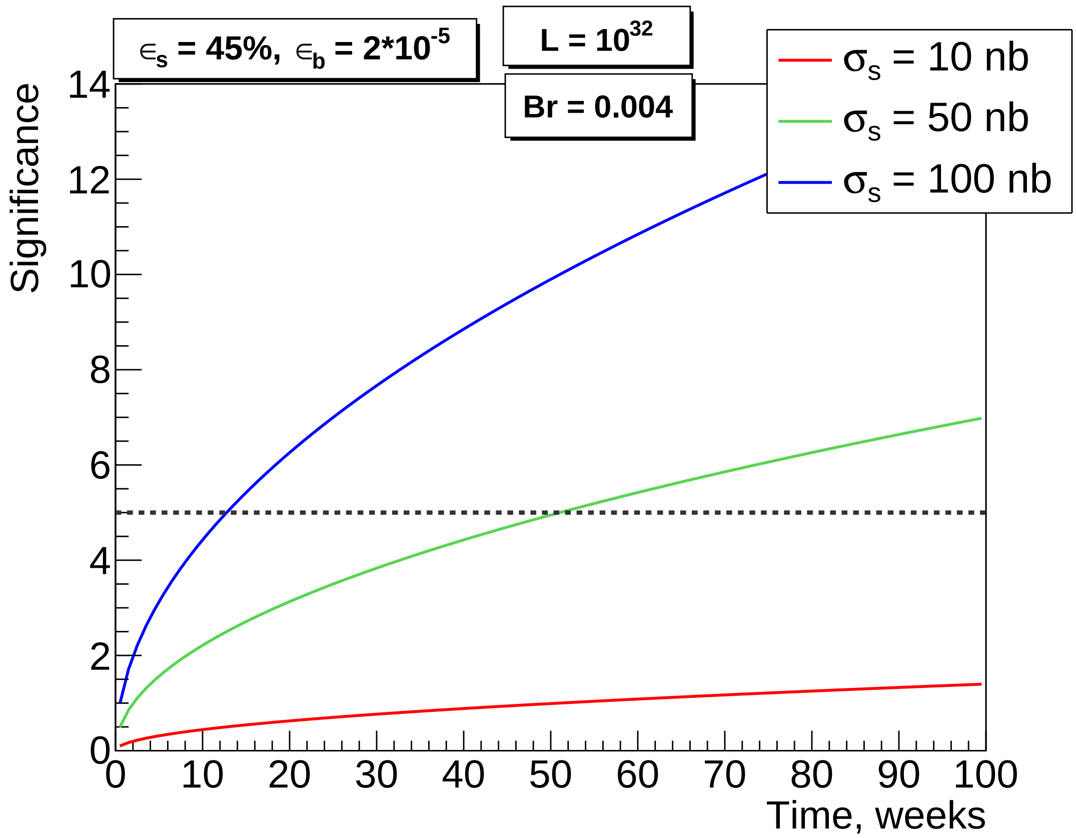


Fig. 22: Significance for $h_c \to 2(\pi^+\pi^-)\pi^0$.
Time for $10^4$ events: 64, 13 and 7 days respectively for 10nb, 50 nb, 100 nb

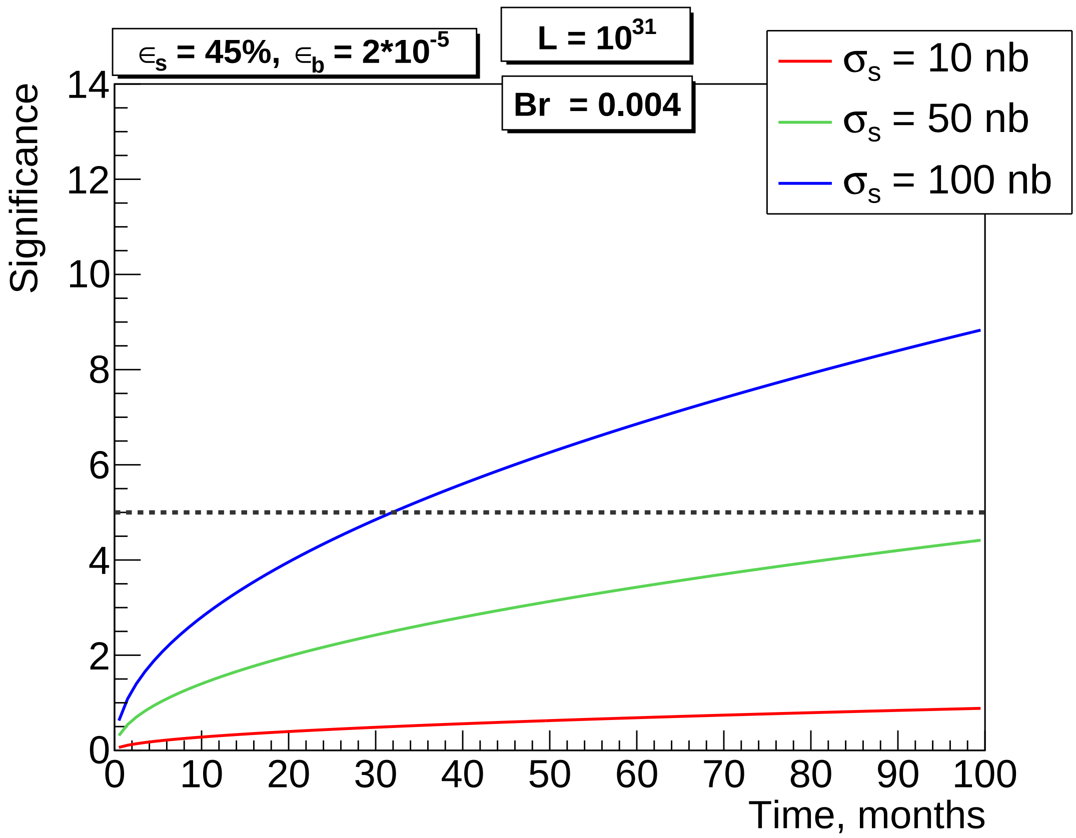


Fig. 23: Significance for $h_c \to 2(\pi^+\pi^-)\pi^0$ with reduced luminosity (L=$10^{31}$).
Time for $10^4$ events: 643, 129 and 64 days respectively for 10nb, 50 nb, 100 nb

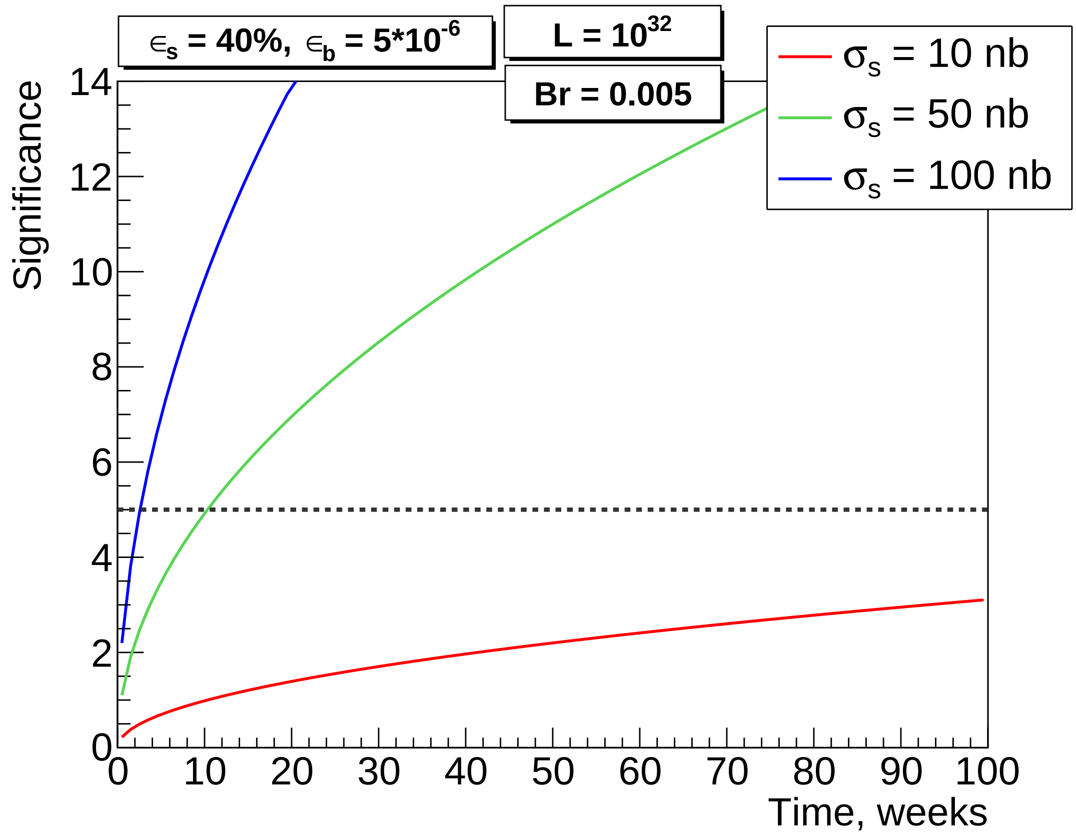


Fig. 24: Significance for $h_c \to \pi^+\pi^-3\pi^0$.
Time for $10^4$ events is 58, 12 or 6 days for 10, 50 or 100 nb respectively

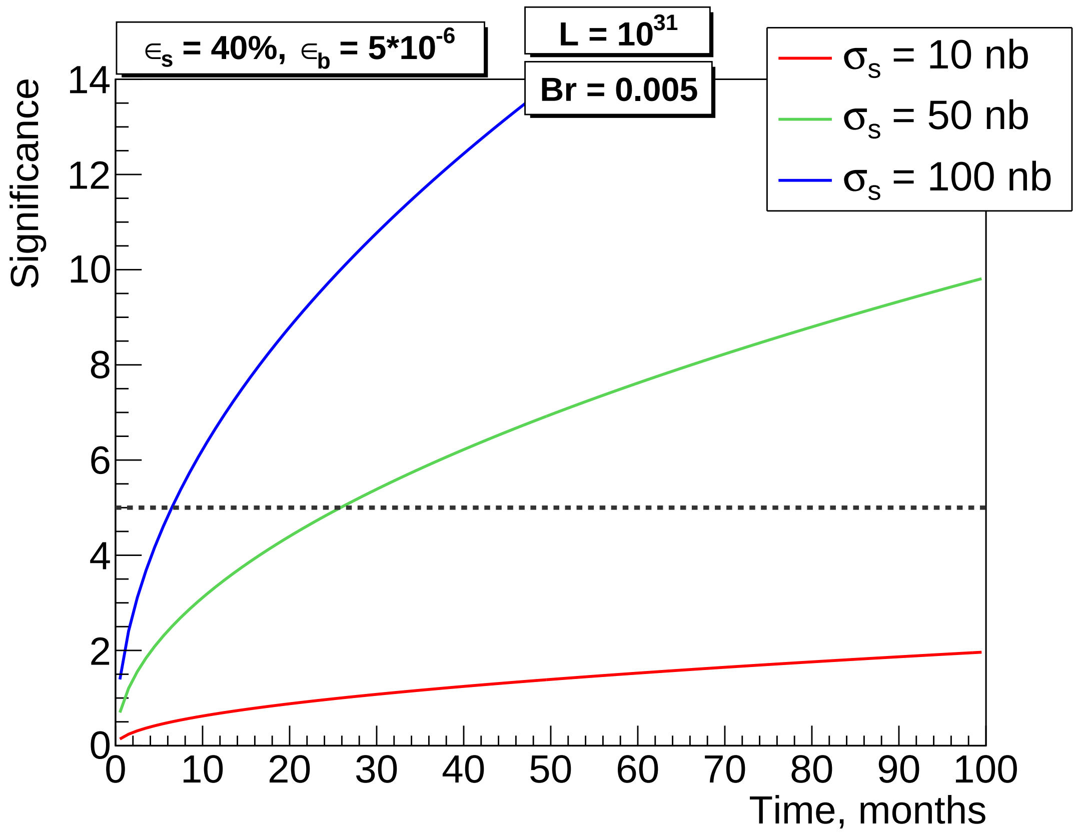


Fig. 25: Significance for $h_c \to \pi^+\pi^-3\pi^0$ with reduced luminosity (L=$10^{31}$).
Time for $10^4$ events is 579, 116 or 58 days for 10, 50 or 100 nb respectivly

## 7 Minimal set-up

Different scenarios were tested as the most relevant for this study (focused almost on EMC), with results shown on Fig. 27 and 26.

1. Full detector
2. EmcBar FwdTrk STT MvdGem
3. EmcBar FwdTrk
4. EmcBar STT MvdGem
5. EmcBar FwdTrk STT
6. EmcBar EmcFwCap FwdTrk STT MvdGem
7. EmcBar EmcFwCap EmcBwCap FwdTrk STT MvdGem
8. EmcBar EmcFwCap EmcBwCap EmcFwd FwdTrk STT MvdGem
9. EmcBar EmcFwd FwdTrk STT MvdGem
10. EmcFwCap EmcBwCap EmcFwd FwdTrk STT MvdGem
11. EmcFwd FwdTrk STT MvdGem
12. EmcFwCap EmcBwCap FwdTrk STT MvdGem

Due to high number of particles in final state and requirement for fully reconstructed event (with all charged and neutral particles) EMC Barrel part is esential for this analysis. Also one should note that with only Barrel spectrometer (scenario 4 in list above) one can already reach half of signal efficiency for both channels. Additional Forward Cap EMC and Forward tracking system increase signal efficiency significantly (scenario 6). And complete EMC with both barrel and forward tracking systems give the highest achievable signal efficiency. One can not expect serious background reduction in reduced scenario, as was shown in previous tests. Also PID doesn't help much, since background with pions in finale state is naturally dominating here. Therefore one can conclude that Disc DIRC, Barrel DIRC and RICH are not important for this measurement. Concerning Forward Spectrometer, one should remember, that model used for analysis didn't include any production mechanism for $h_c$, which could significantly increase importance of Forward part of $\bar{\text{P}}$ANDA.

Tab. 6: Efficiency with different detector set-ups

| Channel | Full | 2 | 3 | 4 | 5 | 6 | 7 | 8 | 9 | 10 | 11 | 12 |
|---|---|---|---|---|---|---|---|---|---|---|---|---|
| $h_c \to \pi^+\pi^-3\pi^0$ | 40.52 | 20.12 | 0 | 18.57 | 6.71 | 32.2 | 33.39 | 40.02 | 20.64 | 1.92 | 0.03 | 0.22 |
| $h_c \to 2(\pi^+\pi^-)\pi^0$ | 42.83 | 23.9 | 0 | 22.9 | 8.78 | 37.43 | 37.52 | 42.98 | 26.66 | 7.85 | 0.85 | 3.9 |

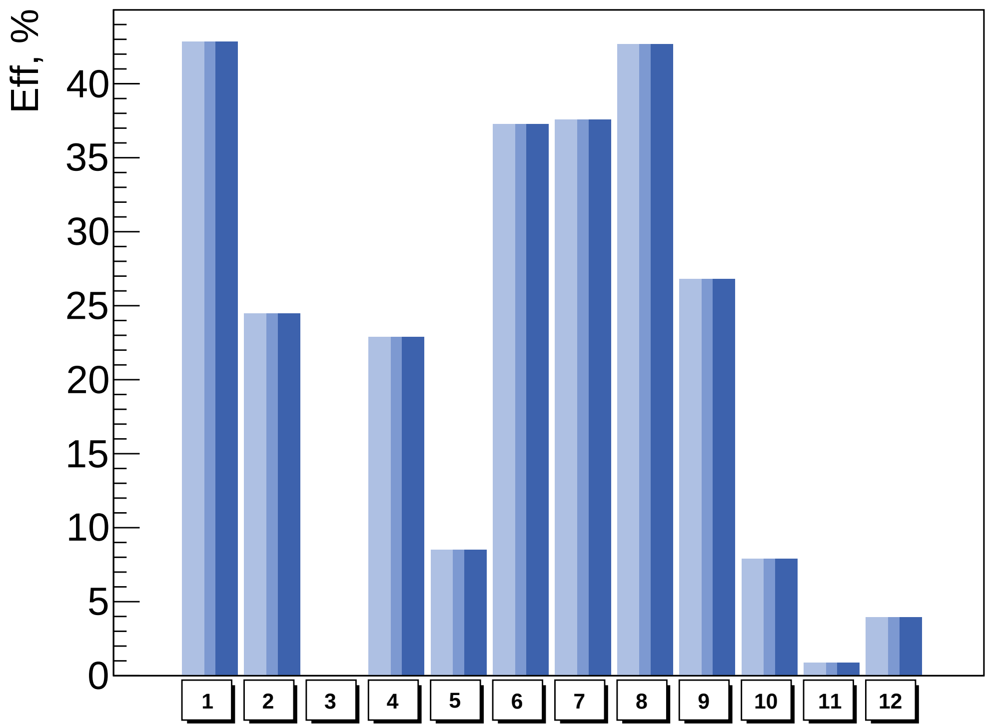


Fig. 26: Efficiency for $h_c \to 2(\pi^+\pi^-)\pi^0$ with different detector set-ups

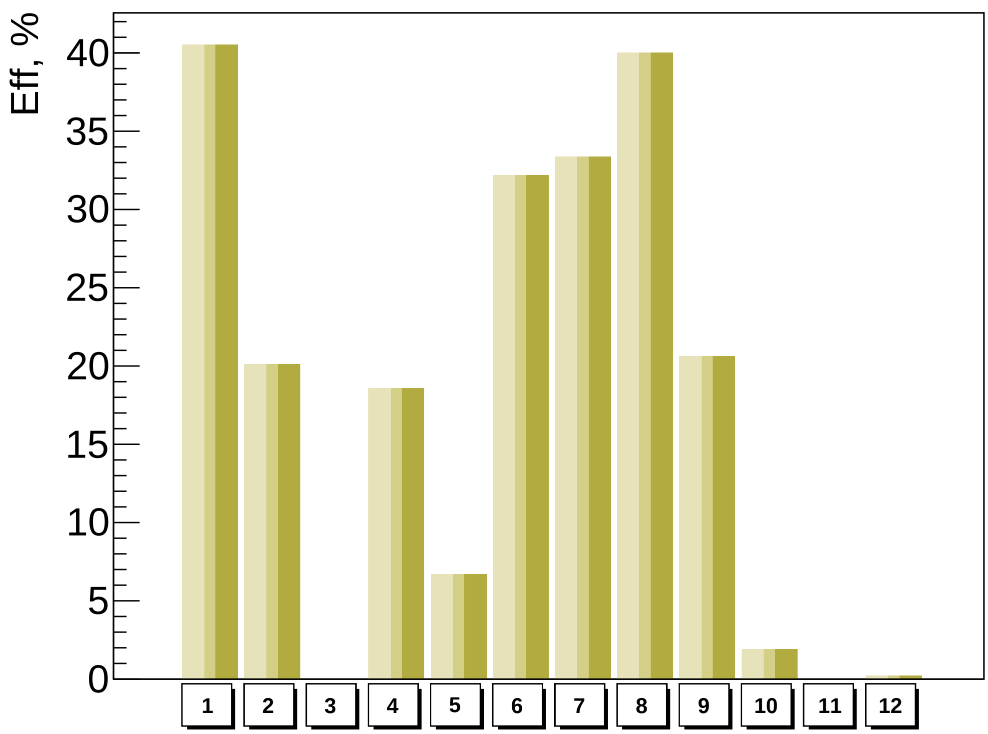


Fig. 27: Efficiency for $h_c \to \pi^+\pi^- 3\pi^0$ with different detector set-ups

# 8 Conclusion

The aim of this preliminary study was to show possibility of measurement of $h_c \to \text{light hadrons}$ decay modes at $\bar{\text{P}}$ANDA. Channel $h_c \to 2(\pi^+\pi^-)\pi^0$ was chosen due to high cross-section of such final state in $\bar{p}p$ interactions. Therefore from background point of view it should be the most challenging one. Indeed to suppress background to some reasonably small fraction some kind of model assumption was needed. In this study very simple (naive) model was tried and suppression of background efficiency $\epsilon_b$ up to $\sim 10^{-5}$ was demonstrated.

Within proposed model of $h_c$ via two body decay it turned out that channel $h_c \to \pi^+\pi^-3\pi^0$ can be described in the same way. For this decay mode background is smaller due to smaller cross-section $p\bar{p} \to \pi^+\pi^-3\pi^0$ in this energy range. Therefore background efficiency $\epsilon_s \sim 10^{-6}$ can be easily achieved. Measuring $h_c \to \pi^+\pi^-3\pi^0$ at $\bar{\text{P}}$ANDA could be the first measurement of this decay mode.

Due to just pions in final state, PID is not very important or helpful for both of considered channels. In case of requirement of all neutral and charged particle registration (complete reconstruction of final state) EMC Barrel and STT turned out to be the most essential systems. The minimal required set-up should contain: EMC Barrel, STT, MVD+GEM. To increase signal registration efficiency EMC Forward Cap and Forward Tracking systems should be added. And by additional EMC Backward Cap and Shashlyk (EMC forward) signal efficiency close to maximum is achievable.

One should note here, that for production of $h_c$ no model was used. The production mechanism of $h_c$ can significantly increase importance of Forward Spectrometer of $\bar{\text{P}}$ANDA as well as change the result in terms of efficiency and time needed to achieve required significance. Concerning the background model, although very general DPM model was used for background simulation, one should be still careful with these numbers too, because estimation of DPM is not really precise one.

# A Production cross-section

$$\sigma_{BW}(\sqrt{s}) = \frac{(2J+1)\cdot 4\pi}{s-4m_p^2}\frac{BR(h_c\to p\bar{p})\Gamma_{h_c}^2}{4(\sqrt{s}-m_{h_c})^2+\Gamma_{h_c}^2} \tag{13}$$

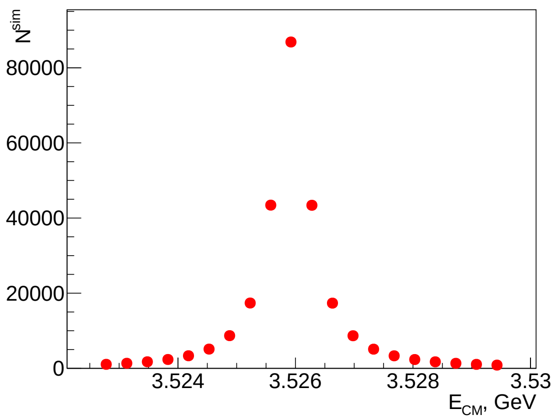


Simulated Breit-Wiegner shape

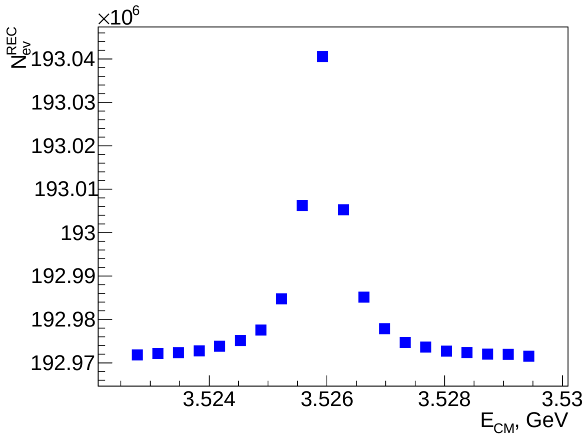


Reconstructed for $h_c \to 2(\pi^+\pi^-)\pi^0$

Fig. 28: Measured rates (red: true distribution, blue: reconstructed signal+ DPM bkg)

Efficiency of reconstruction for $h_c \to 2(\pi^+\pi^-)\pi^0$ and $h_c \to \pi^+\pi^-3\pi^0$ is rather uniform. And without any efficiency corrections resonance shape can be observed (Fig. 28). The reconstructed distribution were not fitted, since work to figure out systematic effects were not done.

# B Reconstruction efficiency

## B.1 Angular distributions

Disributions around $\phi$ are always uniform and therefore not shown in this section

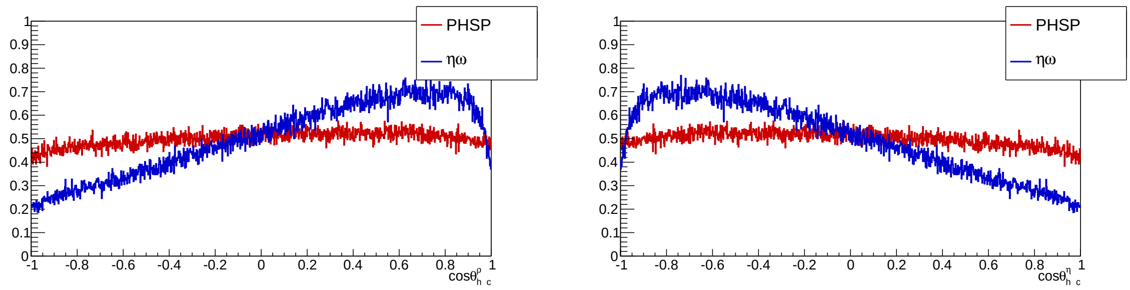


Fig. 29: Angular distributions in rest frame of $h_c$ of reconstructed particles for different models of decay $h_c \to \pi^+\pi^-3\pi^0$ (each normilized to 1 for easy comparison)

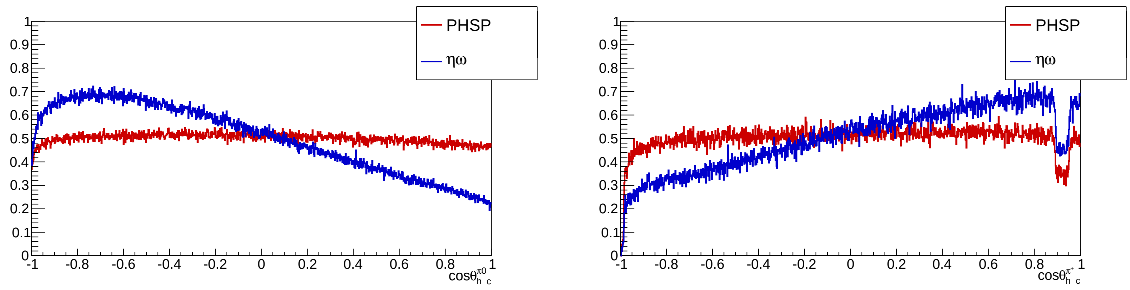


Fig. 30: Angular distributions in rest frame of $h_c$ of reconstructed particles for different models of decay $h_c \to \pi^+\pi^-3\pi^0$ (each normilized to 1 for easy comparison)

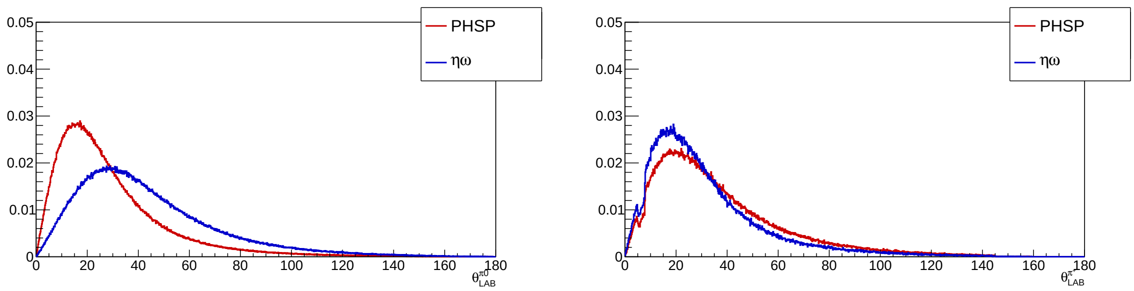


Fig. 31: Angular distributions in LAB frame of reconstructed particles for different models of decay $h_c \to \pi^+\pi^-3\pi^0$ (each normilized to 1 for easy comparison)

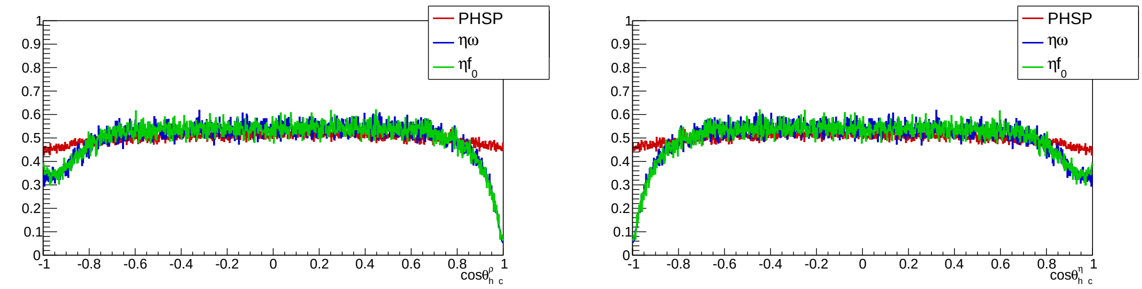


Fig. 32: Angular distributions in rest frame of $h_c$ of reconstructed particles for different models of decay$h_c \to 2(\pi^+\pi^-)\pi^0$ (each normilized to 1 for easy comparison)

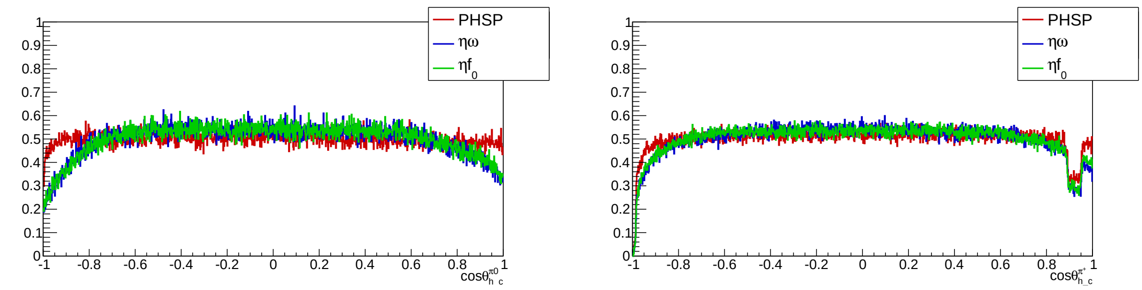


Fig. 33: Angular distributions in rest frame of $h_c$ of reconstructed particles for different models of decay$h_c \to 2(\pi^+\pi^-)\pi^0$ (each normilized to 1 for easy comparison)

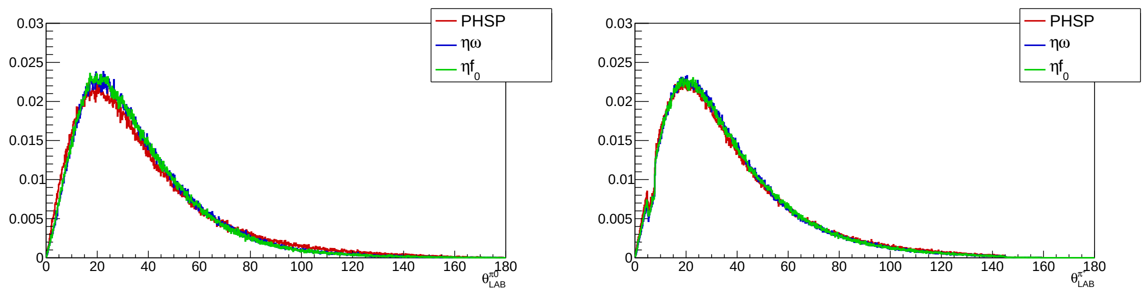


Fig. 34: Angular distributions in LAB frame of reconstructed particles for different models of decay$h_c \to 2(\pi^+\pi^-)\pi^0$ (each normilized to 1 for easy comparison)

## B.2 Efficiencies

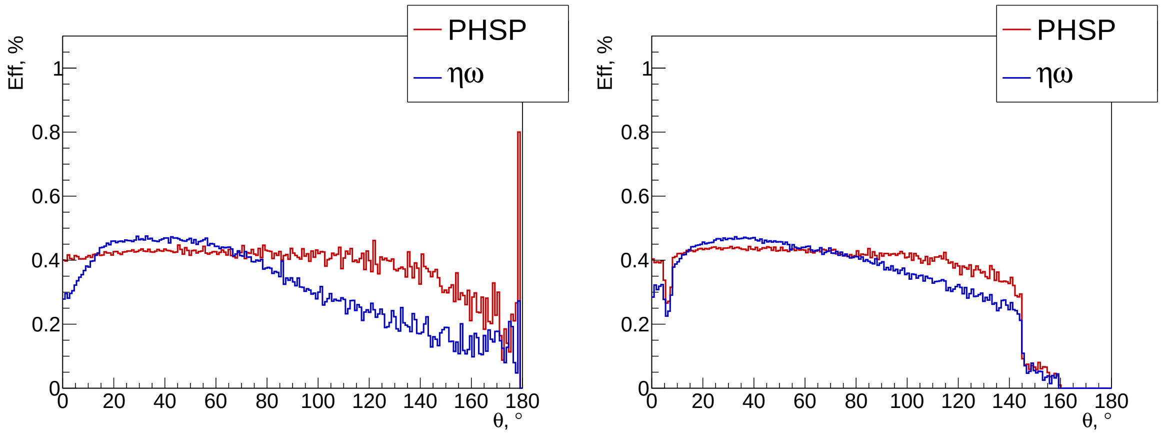


Fig. 35: Efficiency of reconstructed particles in dependence of $\theta_{LAB}$ for different angular models of decay $h_c \to 2(\pi^+\pi^-)\pi^0$

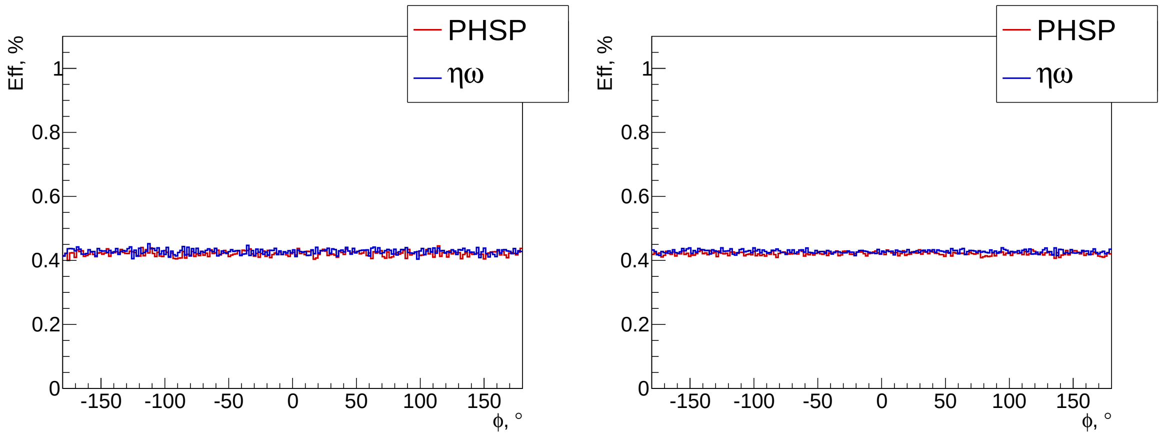


Fig. 36: Efficiency of reconstructed particles in dependence of $\phi_{LAB}$ for different angular models of decay $h_c \to 2(\pi^+\pi^-)\pi^0$

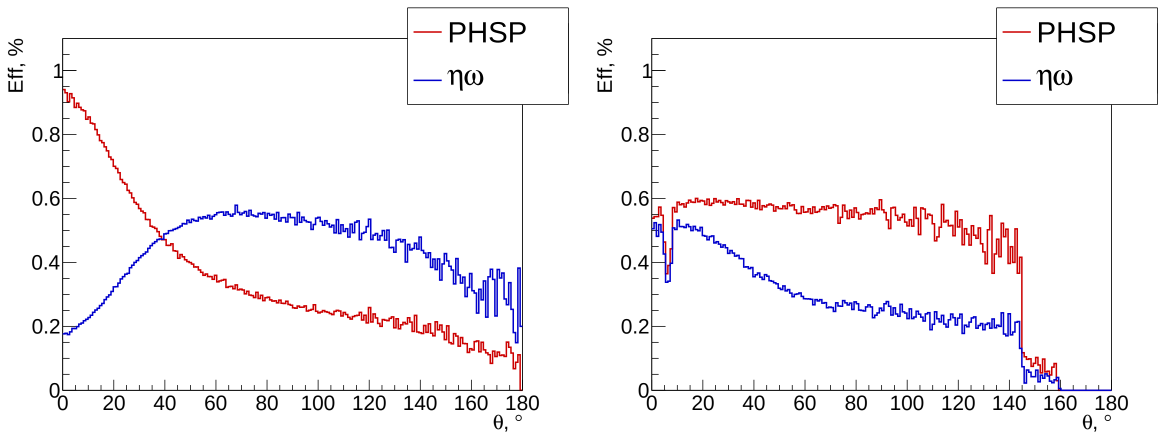


Fig. 37: Efficiency of reconstructed particles in dependence of $\theta_{LAB}$ for different angular models of decay $h_c \to \pi^+\pi^-3\pi^0$

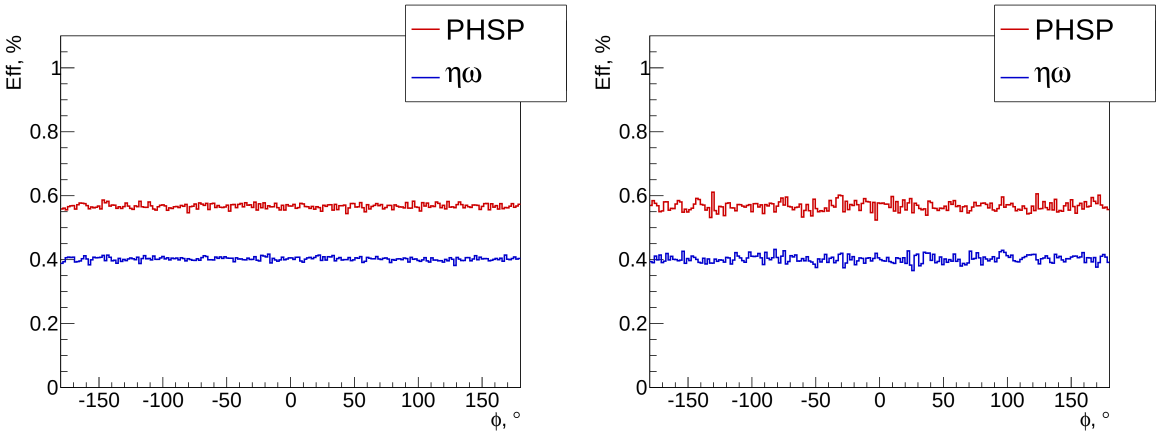


Fig. 38: Efficiency of reconstructed particles in dependence of $\phi_{LAB}$ for different angular models of decay $h_c \to \pi^+\pi^-3\pi^0$

# C Branching ratio measurement

The measurement of branching ratios $\mathcal{B}$ is simple: the total number of events observed in a given final state $N^{obs}_{Q\bar{Q}\to f}$ is proportional to the total number of events produced $N^{prod}_{Q\bar{Q}}$ for that particular resonance:

$$N^{obs}_{Q\bar{Q}\to f} = eff \times N^{prod}_{Q\bar{Q}} \times \mathcal{B}(Q\bar{Q} \to f) \tag{14}$$

where $N^{prod}_{Q\bar{Q}}$ has to be measured by counting some specific events, usually in a "reference" final state $N^{obs}_{Q\bar{Q}\to Ref}$:

$$N^{prod}_{Q\bar{Q}} = \frac{N^{obs}_{Q\bar{Q}\to Ref}}{eff'\mathcal{B}_{Ref}} \tag{15}$$

Then $\mathcal{B}(Q\bar{Q} \to f)$ will use $\mathcal{B}_{Ref}$:

$$\mathcal{B}(Q\bar{Q} \to f) = \frac{N^{obs}_{Q\bar{Q}\to f}}{N^{obs}_{Q\bar{Q}\to Ref}} \frac{eff'}{eff} \mathcal{B}_{Ref} \tag{16}$$

Need of normalization here leads to potential hidden systematic errors, especially in case when measurement for another experiment used as a reference. Providing of ratio of braching rations:

$$R_{\mathcal{B}}(f/f^{'}) = \frac{\mathcal{B}(Q\bar{Q} \to f)}{\mathcal{B}(Q\bar{Q} \to f')} \tag{17}$$

measured at one experiment helps to get rid from normalization and usually from a number of other systematic.

## C.1 Branching ratios and partial widths measured in $p\bar{p}$ formation experiments

A scan of resonance allows direct measurements of mass, total width and $\mathcal{B}(p\bar{p})\mathcal{B}_f$. For resonances whose natural width is comparable or smaller than the beam width, the product $\mathcal{B}(p\bar{p})\mathcal{B}_f$ is highly correlated to the total width and the quantity $\Gamma(p\bar{p})\mathcal{B}_f$ is more precisely determinated. By detecting the resonance formation in more than one final state, the ratio of branching ratios $R_{\mathcal{B}}(f/f^{'})$ can be determined independently from the total width and $\mathcal{B}(p\bar{p})$, in general with small systematic errors since the final state is fully reconstructed, and the angular distribution only depends on a limited number of decay and formation amplitudes. Interference effects with the continuum could affect the measurement of $\mathcal{B}(p\bar{p})\mathcal{B}_f$ and $R_{\mathcal{B}}(f/f^{'})$, but as in $e^+e^-$ experiments, their relevance could be estimated by a measurement of $R_{\mathcal{B}}(f/f^{'})$ across the formation energy of the resonance.

# D Theory expectations

[6] gave following estimation for branching fractions:

$$1^1P_1 \to 1^1S_0\gamma \ (37.7\ \%) \tag{18}$$

$$1^1P_1 \to ggg \ (56.8\ \%) \tag{19}$$

$$1^1P_1 \to \gamma gg \ (5.5\%) \tag{20}$$

According to [7] $\Gamma_{^1P_1 \to \ had}$ ≈120 keV via 3 gluon process. Also there are discussed allowed modes:

- odd number of pions;
  ex: $\pi^+\pi^-\pi^0$ ($\rho\pi$ in S wave)
  $3\pi^0$ is forbidden by C;
- $K\bar{K}$+pions; baryon-antibaryon ($p\bar{p}$,$n\bar{n}$,$\Lambda\bar{\Lambda}$,...)
- $\omega\eta$, $\phi\eta$, ... in S wave; $\omega\epsilon$, $\phi\epsilon$, ... in P wave

For electromagnetic corrections Renald [7] discussed one $\gamma$ + 2 low-energy gluons:

$$^1P_1 \to (\rho, \omega, \phi) + (had)^{C=+1}_{I=0} \tag{21}$$

ex: $^1P_1 \to \rho + (\eta, \eta^{'}, \epsilon, ..)$. One expects here an order of magnitude of $\alpha^2$ time a normal process with two low-energy gluons, e.g $\Gamma_{^1P_1 \to \rho + \eta'} \approx 13$ keV.
(*PDG(1988) contains only one renamed resonance with name $\epsilon$ and it's* $\epsilon(1300) -> f_0(1400)$)

Concerning production in $p\bar{p}$ [7] assumes that $p\bar{p} -^1 P_1$ width is probably similar to $p\bar{p} - \psi$

# E Parameters of models in EvtGen

eta->pi+pi-pi0 as PTO3P
*MAXPDF is the maximum total amplitude (prob density function), summing over all resonances, for the accept reject method: too low, and you will not generate the correct Dalitz plot model; too high and it will waste computing time.*
SCANPDF gives 1.00
*The parameters defined by POLAR_RAD are the magnitude and phase (radians). This means a given resonance will have its dynamic shape multiplied by the constant complex number c = mag*cos(phase) + i mag*sin(phase).*
set to 1.0 0.0

# F Detector model

Scenarios tested to figure out the most important parts of the detector for this study (with results are shown on Fig 39)

1. Full detector
2. only Forward Spectrometer
3. Forward Spectrometer and MVD
4. Forward Spectrometer and GEM
5. Forward Spectrometer and MVD+GEM
6. Forward Spectrometer and Drc
7. Forward Spectrometer and Dsc
8. Forward Spectrometer and backward EMC
9. Forward Spectrometer and forward barrel EMC
10. Forward Spectrometer and barrel EMC
11. Forward Spectrometer and full barrel EMC
12. Forward Spectrometer and Barrel MUO
13. Forward Spectrometer and STT
14. Barrel Spectrometer
15. Barrel Spectrometer and forward EMC
16. Barrel Spectrometer and full Forward Tracking
17. Barrel Spectrometer and RICH
18. Barrel Spectrometer and forward MUO

Please, note on Fig.39 efficiencies for $h_c \to \pi^+\pi^- 3\pi^0$ should be divided by factor ~2.

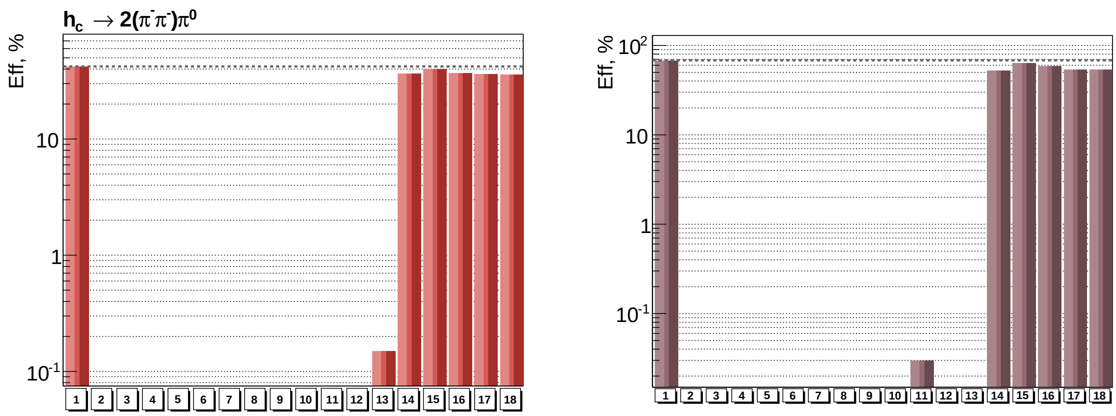


$h_c \to 2(\pi^+\pi^-)\pi^0$ $\quad$ $h_c \to \pi^+\pi^- 3\pi^0$

Fig. 39: Efficiency with different detector set-ups

## References

[1] PDG web page (status of April 2014)

[2] E. Eichten et al "Quarkonia and their transitions”, arXiv:hep-ph/0701208

[3] QWG report "Heavy quarkonium physics" arXiv:hep-ph/0412158

[4] A. Dbeyssi, E. Tomasi-Gustafsson "Classification of $\bar{p} + p$ induced reactions", Problems of Atomic science and technology (2012) **N 1**

[5] arxiv:0906.4470

[6] arXiv:hep-ph/0205255

[7] F.M.Renald "How to produce and observe the $^1P_1$ charmonium state?", Phys.Lett. (1976) **65B**

[8] EvtGen user guide